A GRAVITY SURVEY OF EASTERN NOTRE DAME BAY, NEWFOUNDLAND

HUGH G. MILLER, B.Sc. (HONS.)

C.1

A GRAVITY SURVEY OF EASTERN NOTRE DAME BAY, NEWFOUNDLAND

by

© HUGH G. MILLER, B.Sc. (HONS.)

"Submitted in partial fulfilment
of the requirements for the degree of Master of Science,
Memorial University of Newfoundland.

July 20, 1970"

ABSTRACT

A gravity survey was undertaken on the archipelago and adjacent coast of eastern Notre Dame Bay, Newfoundland. A total of 308 gravity stations were occupied with a mean station spacing of 2.5 km, and 9 gravity sub-bases were established. Elevations for the survey were determined by barometric and direct altimetry. The densities of rock samples collected from 223 sites were determined.

A Bouguer anomaly map was obtained and a polynomial fitting technique was employed to determine the regional contribution to the total Bouguer anomaly field. Residual and regional maps based on a fifth-order polynomial were obtained. Several programs were written for the IBM 360/40 computer used in this and model work.

Three-dimensional model studies were carried out and a satisfactory overall fit to the total Bouguer field was obtained. Several shallow features of the anomaly maps were found to correlate well with surface bodies, i.e. granite or diorite bodies. Sedimentary rocks had little effect on the gravity field. The trace of the Luke's Arm fault was delineated.

The following new features were discovered: (1) A major structural discontinuity near Change Islands; (2) A layer of relatively high density (probably basic to ultrabasic rock) at 5 - 10 km depth.

CONTENTS

CHAPTER 1

INTRODUCTION

The subject of this thesis is a gravity survey of eastern Notre Dame Bay, Newfoundland. The total area covered is approximately 2500 km^2, bounded by latitudes $49^{o}00'N$ and $49^{o}50'N$ and longitudes $54^{o}00'W$ and $55^{o}30'W$.

1.1 Geology

The area is part of the Paleozoic Mobile Belt of Newfoundland (Williams, 1964). An examination of any geological map shows that the basic structural trend in the area is north-easterly. The area is one of the few where a mountain system cuts the continental margin at a right angle. Major deformation of the rocks in the area occurred during both the Taconic and Acadian orogenies. Mafic, ultramafic and granitic material was intruded into the existing rocks during the Taconic orogeny, i.e. late Ordovician. In this region the Silurian was a relatively quiet period during which there was some volcanic activity. The sediments of this period are shallow-water type, the most prominent being the thick conglomerate sequences. The most intense orogeny affecting the region occurred during Devonian times. During this period most of the granitic material exposed in Notre Dame Bay was intruded. Since the Devonian, the area has remained stable (Fig. 1.1).

1.2 Geophysical Work

The area has been well studied geologically. However, standard geological methods apply only to surface rocks, whereas the most interesting problem related to the Paleozoic Mobile Belt concerns its composition and shape near the continental margins; here geophysical methods must be used exclusively, at least in the region beyond the islands of the Bay of Exploits.

Much interest today is centered around theories of continental drift. The reconstruction of the North Atlantic by Bullard et al. (1965) places the continental shelves of Europe and North America adjacent to one another, much as Wegener (1921) proposed, though more recent evidence favours an earlier date than Wegener's for the initiation of the opening of the North Atlantic. Either of these reconstructions is consistent with the proposition that the Caledonian system of Great Britain and the Appalachian system of North America were once a single system. If this hypothesis is accepted, the area northeast of the Bay of Exploits should provide evidence about the location of the break in the Appalachian-Caledonian system, i.e. the Appalachian structure would be continuous to the continental margin, where it would abruptly end. If the system is not continuous to the continental margin, then it becomes more difficult to accept the hypothesis of continuity of the Appalachian-Caledonian system. Seismic and magnetic data should provide important information about the structural trends towards the continental margin.

1.2.1 Shipborne Geophysical Surveys. The above postulates have been tested by Dalhousie University (Ewing et al., 1966), Bedford Institute of Oceanography (Fenwick et al., 1968), and Lamont Geophysical Observatory (Sheridan and Drake, 1968). From results obtained on two sets of seismic refraction profiles (one set each transverse and parallel to the continental shelf), located in an area between Fogo Island and about 60 kilometers northeast of that island, the Lamont group concluded that the Taconic orogenic belt extends to the continental margin with no change in axial direction. Since the Appalachian and Caledonian systems were both affected by the Taconic orogeny, while the effects of the Acadian orogeny are observed only in the Appalachians and appear to die out short of the continental margin, they further conclude that there is a significant crustal discontinuity at the shelf edge of post-Taconic, pre-Acadian age. The chief evidence for these conclusions is the presence of a high-velocity (6.68 - 7.30 km/sec) intermediate layer at depths varying from 4 to 8 kilometers on the profile running transversely to the shelf from Fogo Island outward. The depth to this layer is about 8 kilometers on the profile parallel to the shelf. Sheridan and Drake assume this layer is basic to ultrabasic rock associated with the Taconic orogeny. These conclusions elucidate the findings of Ewing et al. (1966).

Since the intermediate layer is basic it should produce positive magnetic anomalies. A series of magnetic and refraction seismic profiles were run parallel to the shelf by Bedford Institute (Fenwick et al. (1968). The seismic results agreed with those of Sheridan and Drake, and the magnetic results showed an anomaly pattern with contours parallel to the shelf edge, and with the amplitude decreasing towards deeper water. The

authors interpret this as evidence for the abrupt discontinuity at the continental margin where the thicker continental crust with the intermediate layer grades into oceanic crust with a thin basaltic layer. From these results it appears that the Appalachian system is continuous to the continental margin from the sea-ward extremity of the present survey area. Among the most interesting features one could hope to detect is the basic to ultrabasic layer at a depth between 4 and 10 km.

1.2.2 Previous Gravity Work

The only published gravity work carried out in the area of the present survey is the Dominion Observatory survey of Newfoundland (Weaver, 1967), in which the station spacing was 10 to 13 kilometers with seventeen stations in the present survey area. The results show a rapid change from low to high anomalies, predominantly in a direction perpendicular to the geological strike, including two or three prominent features. Weaver's main conclusions are (i) that diorite and gabbro cause the large positive anomalies, and (ii) that in the case of Newfoundland, sedimentary rocks do not have much effect on the gravity field. Since the station spacing of the Dominion Observatory survey was large, several important features could not be accurately outlined, thus justifying the need for a survey with closer station spacing in the area of rapid change and critical importance for the geophysics of the Appalachians.

1.3 Present Survey

The present survey was conducted during July 1968 and May to August 1969. Gravity and elevation determinations were made for

308 stations, and 9 gravity sub-bases were established. The principal facts for these stations and sub-bases are given in Appendices 1A and 1B. The mean station spacing was 2.5 km, with stations being set up on the existing roads and on islands in the Bay of Exploits and Dildo Run, as well as Change Islands and Fogo. The station spacing was adopted on the basis of a desire to obtain more detailed gravity information than available, and by considering the geography of the area. Base stations were tied to one another according to standard procedure (Section 3.1), the whole grid being tied to the Dominion Observatory base 9001 at Bishop's Falls, Newfoundland.

Transportation was by Jeep and Land Rover on roads, and by boats rented from local fishermen for islands in the Dildo Run, Bay of Exploits, and Cobb's Arm areas. The bases at Cobb's Arm and Fogo were tied together by aeroplane. Distances along the roads were determined from the odometer of the vehicle used. This was checked periodically and found to be accurate to 0.08 km. The island station locations were determined with the aid of 1:50000-scale topographic maps of the Department of National Defence. All station positions are known to ± 0.05'latitude or approximately 100 m.

Elevations were obtained by direct levelling and barometric altimetry (Chap. 2). Direct levelling was used for 159 stations and all barometric altimeter bases. The remaining 149 stations were determined by barometric altimetry.

Density control was obtained by sampling as many outcrops as possible (Chap. 4). A total of 223 samples was collected.

(See Fig. 4.1 DENSITY DISTRIBUTION at end of document.)

CHAPTER 2

MEASUREMENT OF ELEVATION

Elevation is one of the most important parameters determining the ultimate precision of any gravity survey. To achieve an error less than 0.4 mgal (1 mgal = 10^{-3} cm/s^2) in the Bouguer anomaly (Section 3.3) one must know the elevation within 2 meters. The efficient determination of elevation to such an accuracy is a major problem. Elevations for this survey were determined by barometric altimetry and direct levelling.

2.1 Direct Levelling

Direct levelling is the more precise but slower method. For this reason it was used in determining elevations on islands or near the sea, where few set-ups of the level were required. This method was also used in determining reference elevations for use with barometric altimetry.

The accuracy of direct levelling is determined by the precision of the instruments and the technique chosen, and is limited by the personal errors of observation. A standard level with tripod stand was used with a standard 13-ft. collapsible rod. Shot distances were 50 m or less. At this distance the maximum reading error due to mis-levelling the instrument was about 1.0 cm for a single shot. Thus for a single forward and backward shot, the expected error is about 1.4 cm. For any levelling requiring more than one set-up, i.e. more than one forward and one backward shot, the error is $(2n)^{\frac{1}{2}}$ cm, where n is the number of times the level was set up.

In obtaining an elevation by direct levelling, sea-level at the time of the first shot was usually taken as the reference, except in cases where bench marks were available. All elevations were referred to a standard datum plane (Section 2.1.1). Since sea-level has a regular diurnal and semi-diurnal variation due to tides, the arbitrary sea-level readings may be standardized by applying a correction found from tide tables. Sea-level also has an irregular variation due to meteorological effects which cannot be calculated. However, work was not carried out during periods of high wind or adverse sea conditions, so that it is safe to assume that meteorological effects were also negligible.

2.1.1 Tidal Corrections. The major corrections for directly levelled elevations arise from tidal factors. The first problem in applying tidal corrections is the choice of a datum plane to which all elevations can be referred, with the condition that no elevation will be negative, i.e. below the datum plane. Since the elevations of several stations were determined near low tide, the datum plane should not be higher than the low-tide water level. One such plane in common usage is "Chart Datum"[1], defined as the plane below which the water level seldom, if ever, falls. All elevations in this survey are referred to this plane. It would have been simple to refer all elevations to mean sea-level, which is the standard datum for gravity work, if the difference between Chart Datum and mean sea-level had been known for the entire area.

---

[1]Hydrographic Tidal Manual, 1969 Edition. Hydrographic Service of Canada, Ottawa, 142 p: ref. p. 80.

Let us now consider the magnitude of the necessary corrections for tidal variation. Data from tidal tables[1] for four ports with respect to St. John's, Newfoundland, are given in Table 2.1. This shows the time and height terms to be added to St. John's predictions to give the predicted water levels at the respective ports, based on mean tide variations for each port.

In making a tidal correction the data of Table 2.1 are used as outlined by the Hydrographic Service of Canada. However, some modification to these techniques had to be devised, since Table 2.1 enables one to make corrections only for the four ports listed. For actual stations the tidal correction to the high and low water values of Table 2.1 was obtained by linear interpolation between appropriate values of that table.

To obtain an estimate of the error involved with this method, consider Lewisporte, which is situated about one-third of the distance from Botwood to Exploits Harbour. The high-water correction based on linear interpolation between Botwood and Exploits is + 0.21, agreeing fairly well with the true value + 0.23 m for Lewisporte given in Table 2.1. Similarly, the table gives + 0.16 m and + 0.13 m, respectively, for the low-water linear interpolation and the true Lewisporte correction. The error for both high-water and low-water correction is small enough to justify the application of this method to any station between Botwood and Exploits Upper Harbour as far east as the Dildo Run.

---

[1] Canadian Tides and Currents, 1968 and 1969 editions, Volume 1, East Coast and Bay of Fundy. Hydrographic Service of Canada, Ottawa.

A similar technique was applied to stations and altimetry bases on the open Atlantic between Exploits and Fogo. Here, however, no port was available for which the technique could be tested, so that the error may be as large as the difference in the correction value from Table 2.1 for Fogo and Exploits, i.e. 0.39 m for high water and 0.33 m for low water. These latter errors apply to stations on Change Islands, near Cobb's Arm, and to barometric altimetry bases at Herring Neck, Twillingate Ferry terminals, Virgin Arm, Moreton's Harbour and Toogood Arm. At the altimetry bases, the uncertainty due to the absence of reference ports results in increased uncertainty at all stations run from these bases. This will be further discussed in Section 2.2.

The second error having an effect on the tidal correction arises from the difference in duration of the tidal period at different ports. The most extreme case is at Botwood, where the duration is 23 minutes shorter for a high tide to the next low tide, and 23 minutes longer for a low tide to the next high tide, than for St. John's. In order to estimate the error for a wrong choice of port, hence a wrong duration value, the range tables and duration tables must be used. Table 2.1 shows that the maximum change in the range for any port differs by only 0.10 m from the range at St. John's. As the mean tide range for St. John's is 0.9 m and durations are given in the tables to the nearest 10-15 minutes, the maximum error one could make in the range duration tables is of the order of 0.03 m.

From this discussion it is obvious that the main source of error in directly levelled stations arises from the linear interpolation for stations on the open Atlantic. Here the error may be as great as 0.4 m,

which would cause an error of 0.08 mgal in the Bouguer anomaly. For stations in the sheltered portion of the survey area, the limit of error from direct levelling and tidal corrections is $0.03 \text{ m} + (2n)^{\frac{1}{2}}/100 \text{ m} + 0.03 \text{ m}$. For a single set-up of the level this is 0.07 m corresponding to an error in the Bouguer anomaly of < 0.02 mgal.

2.2 Barometric Altimetry

The second method of elevation measurement used in this survey was barometric altimetry. The basic instrument is an aneroid barometer calibrated in feet. With this instrument the elevation difference between a known elevation and a station of unknown elevation may be measured. This difference must be corrected for temperature and humidity using tables.

2.2.1 Method. In this survey the so-called "modified single-base method"[1] was used, employing four Wallace and Tiernan FA-181 altimeters, three having ranges 0-4000 ft., and the fourth 1000-5000 ft. No calculations were based on the 1000-5000 ft. instrument, which had a reading accuracy corresponding to ± 0.30 m compared with ± 0.15 m for the other instruments. Two of the 0-4000 ft. instruments were used for roving on traverses, while the third remained at base; thus each traverse yielded two elevation differences, Δh, between the base and any station. These two differences, after correction for temperature and humidity, were each added to the base elevation, and the arithmetic mean of the two sums was taken as the elevation of the station for the traverse concerned. Each

[1] Altimeter Manual, Wallace and Tiernan, Inc., Belleville, N. J. (No date given).

traverse was usually run at least twice, using bases established at opposite ends of the traverse. The elevations of a station determined from the various traverses were then treated as discussed in Section 2.2.3.

To estimate the error of this method, elevations were determined by barometric altimetry at points of known elevation. The difference between the known and the barometrically determined elevation is an indicator of the error involved. The comparison was usually made first at a "known" station at the opposite end of the traverse from the base (also "known"); when the traverse was repeated for the same set of stations with the previous "known" station as base, the previous base was used as the check-point. If the two traverses were run on the same day, such that the weather system had not changed in character, one would expect the difference between the true and barometric elevations at the two "known" stations to be equal in magnitude, but opposite in sign. Assuming that enough traverses were run in different directions and under varying weather conditions, one would also expect the mean difference, between the true and barometric elevations based on all sets of comparisons, to be close to zero. Using the data from the 54 check-points employed, it was found that $\bar{x} = -0.25$ m with a standard deviation of $\pm$ 1.8 m. A t-test showed that this mean was not significantly different from zero at the 95% confidence level.

2.2.2 Weighting. These statistics must be reconciled with the actual traverse data. Thus, in determining an average elevation for a station from the data for all traverses which included that station, it is useful to apply some procedure making use of the "check-in difference",

x, defined by $x = \Delta h - \Delta h_b$. Here Δh is the true elevation difference between the two known stations (usually terminal) for a given traverse and Δh_b the barometrically determined elevation difference between the same stations. A weighting scheme was devised based on (i) the absolute value of the check-in difference, and (ii) the station location on a traverse.

In Figure 2.1, let the station elevations be determined once on each of two traverses, AB and BA, having A and B as bases, respectively. If h_A, h_B are the elevations of A and B from barometric altimetry, then the difference, $\Delta h_b = h_B - h_A$, obtained on the first run, AB, differs by the check-in difference, x, defined above from the true Δh. The second run, BA, should yield a check-in difference, -x, if the same weather conditions prevailed. Repeated observations seem to bear out this conclusion. If, however, the weather conditions were not the same, then the repeat value of x will tend to differ in magnitude and possibly in sign from the expected value -x.

An easy but incorrect way of determining station elevations would be to compute the arithmetic mean of the values obtained for a given station on traverses, AB and BA, where the error may be estimated from the associated check-in difference, x and y, assuming y = -x. This mean elevation would be too high near B, where the error from the first run would be greatest, and too low near A, if it is assumed that the error increases with distance from base. If one overweights the stations near A on the first traverse, and near B on the second traverse, this error may be reduced. Hence, an arbitrary scheme was adopted in which

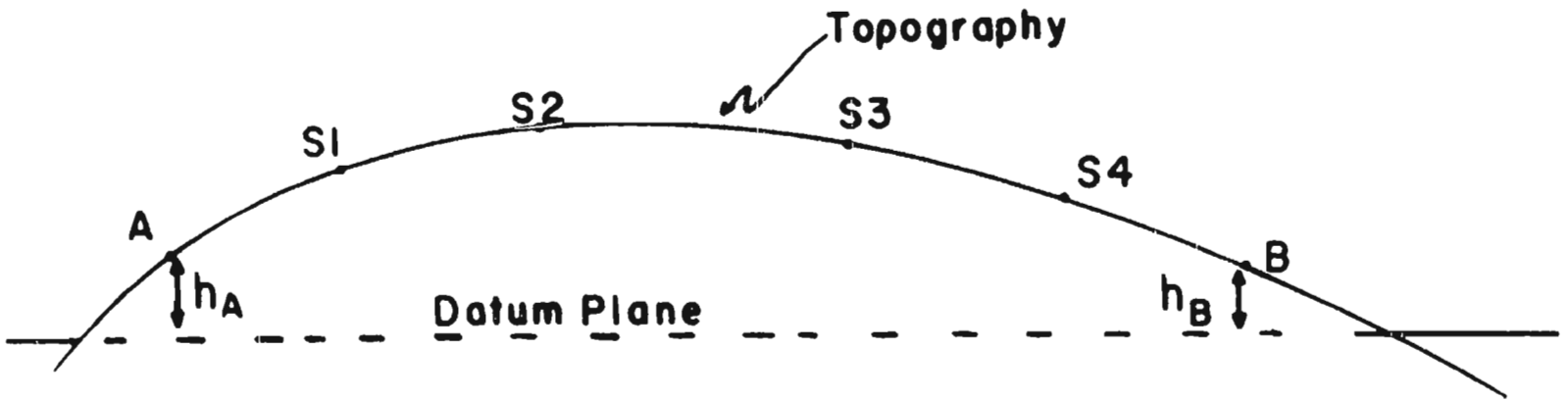

Datum Plane – Chart datum (Section 2·1·1)

A, B – Base stations - elevations from direct levelling

h_A, h_B – Elevations of bases A, B

S1-S4 – Station elevations to be determined by barometric altimetry

Fig. 2·1 Schematic View of Barometric Altimetry Traverse

weights in the ratio 3:2:1 were assigned to the three-thirds of the traverse, starting from A in traverse AB and from B in traverse BA.

The positional weighting above is independent of the check-in difference for which a separate weighting scheme based on check-in statistics was devised. The weights are the probabilities of getting a check-in difference exceeding in magnitude the minimum value in the appropriate range shown in Table 2.2 (first column), the probabilities being based on a normal curve (last column), with mean $x = -0.25$ m and standard deviation 1.8 m. For comparison, a weighting scheme devised from the frequency of occurrence of various check-in differences is shown in the third column. The data in the first column correspond to values of $|x|$ that were originally obtained in feet on the altimeter scales. Thus the value in the first row (< 0.30 m) corresponds to 1 ft., which is the magnitude of the probable error for a station elevation. The ranges in the second (0.30 - 0.60 m) and subsequent rows correspond to $|x|$ values of 1-2 ft. (considered good), and then in 2-ft. intervals to 10 ft. (3.0 m) which is considered a bad check-in.

The weights based on the normal curve are combined with the traverse weights and applied to the relevant elevation data to give a more realistic mean elevation for a station than would have been obtained by computing the unweighted arithmetic mean.

2.3 Accuracy of Elevations

Using the weighting scheme of Section 2.2.2, the station elevation is given by

$$\bar{h} = \frac{W_{T1}W_{C1}\bar{h}_1 + W_{T2}W_{C2}\bar{h}_2}{W_{T1}W_{C1} + W_{T2}W_{C2}} \qquad (2.1)$$

where the error in $\bar{h}$ may be written as

$$\varepsilon(\bar{h}) = \pm \left| \frac{W_{T1}W_{C1}x + W_{T2}W_{C2}y}{W_{T1}W_{C1} + W_{T2}W_{C2}} \right| \qquad (2.2)$$

and where in 2.1 and 2.2

$\bar{h}_1$, $\bar{h}_2$ station elevations determined from the first and second traverse, respectively;

W_{C1}, W_{C2} corresponding weights based on check-in differences;

W_{T1}, W_{T2} corresponding position weights;

x, y corresponding check-in differences.

To illustrate the use of the weighting scheme, consider in Figure 2.1 an example for station S4, which lies on the last third of traverse AB:

Assume the check-in difference for traverse runs, AB and BA, to be x = 0.8 m and y = - 0.8 m, respectively, and the mean elevations for S4, based on two roving instruments, to be 10 m and 8 m, respectively. Then the position weights are W_{T1} = 1 and W_{T2} = 3, and the check-in weights are $W_{C1} = W_{C2}$ = 0.63 (Table 2.2). From equations (2.1) and (2.2) one obtains

$$\bar{h} = 8.5 \text{ m} \quad \text{and} \quad \varepsilon(\bar{h}) = \pm 0.4 \text{ m} \quad .$$

Using the arithmetic mean, one would have obtained $\overline{h}$ = 9.0 m and $\varepsilon(\overline{h}) = 1.0/(2)^{\frac{1}{2}} = 0.7$ m (= maximum deviation from the mean divided by the square root of the number of readings).

For the example chosen, the elevation $\overline{h}$ is correctly biased towards that value having the greater position weight. At the centre of the traverse, $\overline{h}$ becomes the arithmetic mean and $\varepsilon(\overline{h}) = 0$ if $x = -y$. For cases where $|x| \neq |y|$, the elevation will be biased towards the greater value of the weight product.

This weighting scheme gives a method of classifying the barometrically determined elevations. A "good" barometrically determined elevation is one for which the error calculated by (2.2) is less than one standard deviation, as determined from the check-in statistics, i.e. $|\varepsilon(\overline{h})| < 1.8$ m. By combining this error with the tidal errors for the bases (Section 2.1), five classes of elevation may be defined (Table 2.3).

On the basis of the above analysis, it appears that an upper limit on elevation errors is about 3 m. This corresponds to an error in the Bouguer anomaly of 0.6 mgal. Since more than 80% of the stations fall into one of the error classes 1, 2 and 3 (Table 2.3), the most probable error for the survey is much smaller than this. Thus, for over 80% of the stations, the objective of a 2 m or smaller error in elevation has been achieved.

TABLE 2.1

MEAN TIDE DIFFERENCES RELATIVE TO ST. JOHN'S

Port	High Water		Low Water	
	Time (min)	Corr. (m)	Time (min)	Corr. (m)
Botwood	+ 10	+ 0.33	- 13	+ 0.26
Fogo, etc.	+ 05	+ 0.36	+ 07	+ 0.30
Exploits Harbour	00	- 0.03	+ 02	- 0.03
Lewisporte	00	+ 0.23	+ 01	+ 0.13

TABLE 2.2

ELEVATION WEIGHTING SCHEMES BASED ON REPEATED RUNS[1]

Magnitude of check-in difference[2](m)	Frequency (out of 54)	Weight based on	
		Frequency	Normal Curve
< 0.30	10	1.00	1.00
0.30 - 0.60	11	0.82	0.74
0.60 - 1.2	9	0.61	0.63
1.2 - 1.8	8	0.45	0.42
1.0 - 2.4	5	0.30	0.25
2.4 - 3.0	7	0.20	0.14
> 3.0	4	0.07	0.07

[1]Based on a total of 54 check stations.

[2]Defined in Section 2.2.2.

TABLE 2.3

CLASSIFICATION OF ELEVATION ERRORS

Class	Type and range of errors	No. of Stations in class
1	Direct Levelling < 0.15 m	102
2	Direct Levelling 0.15 m - 0.4 m	55
3	"Good" barometric error 0.4 m - 2.0 m	85
4	"Poor" barometric error 2.0 m - 3.0 m	32
5	No check-in on barometric traverse Error = $(\text{max.dev}^{n}.)/(2)^{\frac{1}{2}}$	34

CHAPTER 3

GRAVITY REDUCTION

Interpretation of gravity data requires that adjustments be made to the observed gravity to reduce all values to a common datum plane. These adjustments incorporate the shape and mass of the earth, the elevation of the station with respect to a datum plane, and the attraction due to the material between the station and the datum plane.

3.1 International Gravity Formula

The first adjustment is for the regular part of the earth's gravity field. At mean sea level, the gravitational attraction is defined by the International Gravity Formula (1930),

$$\gamma(\phi) = 978.0490\ (1 + 0.0052884\ \sin^2\phi - 0.0000059\ \sin^2 2\phi)\ . \quad (3.1)$$

The only source of error in this equation which can cause an error in an anomaly is in the latitude. Since the latitude (49^o - 50^oN) is determined to within 0.05 minutes (Section 1.3), this error is less than 0.08 mgal[1].

3.2 Elevation Corrections

The second and third adjustments to the observed gravity values can be combined. The second adjustment accounts for the decrease of gravitational attraction with distance from the centre of the earth.

[1]Tables of Theoretical Gravity between Latitudes 40^o and 80^o at tenth-minute intervals, compiled by J. G. Tanner, Dominion Observatory, Ottawa, 1962 (Unpublished Manuscript).

Since elevations are expressed relative to a datum plane, this adjustment must be added to the observed gravity. It can be shown that the magnitude of this "free air" correction is given to sufficient approximation for this survey by

$$\Delta g_F = 2GMh/R_o^3 = 2g_o h/R_o = 0.3086h \text{ mgal} \qquad (3.2)$$

where G = Universal Gravitational Constant;

M = Mass of the Earth;

R_o = Mean radius of the Earth;

h = Elevation above mean sea level in meters;

g_o = Mean gravity at sea level corresponding to R_o.

The third adjustment compensates for the attraction of the material between the station and the datum plane. It can be shown that this adjustment is

$$\Delta g_B = - 2\pi G\rho h = - 0.1119h \text{ mgal} \qquad (3.3)$$

where G, h are defined above;

ρ = mean density of crustal material;

ρ = 2.67 gm/cm^3 usually being adopted;

and where Δg_B is equal and opposite to the "Bouguer plate effect" = $2\pi G\rho h$.

This correction assumes a slab of material (the "Bouguer plate") bounded by two infinite horizontal planes, one being the datum plane, the other being a plane at height, h, above the datum plane. This condition is never met, though it is often approximated with negligible error under actual conditions. When the error is not negligible, another correction

must be made to correct for the departure of the terrain from the ideal case. The terrain correction is given by

$$\Delta g_T = G\int_V \rho z/r^3 \, dv \qquad (3.4)$$

where z = height of terrain relative to station height;

r = radial distance from station to volume element, dv;

and is equal and opposite to the "terrain effect", which is always negative; i.e. hills and valleys surrounding the gravity station both tend to reduce the Bouguer effect, requiring a positive correction when the terrain effect is significant. The terrain effect can be computed by tables (Hammer, 1939), but in the present survey it was always less than 0.2 mgal, so terrain corrections were not used.

3.3 Anomalies

Two gravity anomalies can be defined at a station from equations (3.1), (3.2), (3.3) and the observed gravity.

(1) The free-air anomaly, defined by

$$g_F = g_{OBS} + 2g_o h/R_o - \gamma(\phi) \qquad (3.5)$$

where g_{OBS} = the observed value of gravity;

(2) The Bouguer anomaly

$$g_B = g_{OBS} + 2g_o h/R_o - 2\pi G\rho h - \gamma(\phi) \quad . \qquad (3.6)$$

Equations (3.5) and (3.6) are the working equations for the determination of anomalies.

3.4 Sub-bases

The absolute value of gravity, g_{OBS}, is not directly determined in a survey of this type. The instrument used, a Sharpe Canadian CG-2 gravimeter, can only measure differences in gravity between points. Thus, for the absolute value of gravity to be determined at a station, the absolute value must be known at some reference point. For this survey the primary reference point was the Dominion Observatory gravity base at Bishop's Falls' railway station. A set of 9 sub-bases (secondary reference points) was tied to this base and the individual stations were referred to the appropriate sub-base. The Botwood and Notre Dame Junction bases were tied directly to Bishop's Falls, and the remainder were tied together sequentially as follows: Notre-Dame Junction - Lewisporte - Boyd's Cove - Summerford - Indian Cove - Cobb's Arm - Fogo. Little Burnt Bay and Twillingate Ferry were tied to Notre Dame Junction and Indian Cove, respectively (Appendix 1B and Figure 1.1). These ties were established in ABAB ... ABA-type loops, where A is the earlier station in the sequence. The mean standard error for all sub-bases in this survey was ± 0.03 mgal. A closure error could not be found since the system was not tied to a second known reference.

3.5 Error in Computed Anomalies

3.5.1 Random Errors. Examination of equations (3.5) and (3.6) reveals the following sources of error:

(1) Observational errors. In addition to the sub-base error of ± 0.03 mgal, there is an observational error due to (i) the instrument scale constant, (ii) reading errors and (iii) drift errors. The scale

constant will be discussed under systematic errors. The scale can be read to ± 0.05 major divisions, but the reading is repeatable only to ± 0.2 major divisions. Since the instrument constant is approximately 0.1 mgal/division, these reading errors correspond to ± 0.02 mgal. The observed drift is caused by a combination of earth tidal variation and instrumental drift, which is of thermal and elastic origin. The observed drift over periods as long as six hours was always less than 0.2 mgal/hour. Maximum earth tide amplitudes are 0.24 mgal (Melchior, 1968), so that drift corrections applied linearly could be in error. However, it may easily be shown that the maximum difference between a linear drift and a sinusoidal variation of the earth tides causes an error in the drift correction of less than 0.02 mgal; thus a linear drift can be assumed. The period of most traverses was two or three hours, with one traverse lasting six hours.

The drift of the instrument was assumed to be linear, so that the error in the drift correction is a combination of the observational errors at the base and station. The error in g_{OBS} due to random observational errors is then at least 0.035 mgal (based on two readings at a base and one at the station) and may be as great as 0.05 mgal for long traverses.

(2) Error in the elevation corrections. The Bouguer correction is given by

$$\Delta g_F + \Delta g_B = 2g_o h/R - 2\pi G\rho h = 0.1967h \text{ mgal} \quad . \qquad (3.7)$$

So from Table 2.3 and Chapter 2.3 it is evident that the error is less than 0.4 mgal for 80% of the stations.

The use of a standard density, $\rho = 2.67$ gm/cm^3 introduces another error due to the departure of the true density from 2.67 gm/cm^3; this effects the correction term, $- 2\pi G h \rho$. The largest elevation encountered in this survey is less than 100 m and the greatest density contrast for a block (Table 4.1) is + 0.13 gm/cm^3. Thus, the maximum error from this cause using this data is $\sim$ 0.6 mgal. However, there are relatively few elevations greater than 50 m and the density contrast tends to be smallest where the topography is highest; hence this error usually can be neglected.

(3) Latitude error. The theoretical value of gravity at mean sea level, $\gamma(\phi)$, is known to within ± 0.08 mgal arising from the latitude error of ± 0.05'.

3.5.2 Systematic Errors. In addition to the random errors there are two systematic errors. One is due to the choice of the datum plane and is not an "error", strictly speaking. The second is an instrumental error.

(i) Choice of datum plane. For most gravity work the datum plane is mean sea level, which coincides with the height of the geoid. This is the reference level for the International Gravity Formula. Chart datum was chosen for this survey since corrections for chart datum to mean sea level were not available for all parts of the area (Section 2.1.1). From two bench marks near Lewisporte it is found that mean sea level is 0.70 m above chart datum; thus Bouguer anomalies in the area are about 0.14 mgal higher than would be found by a standard survey. No data was available for comparison between mean sea level and chart datum in other

parts of the survey, but tidal tables suggest that the difference may be roughly the same as that near Lewisporte.

(ii) Instrument scale constant. The second systematic error arises from the instrument constant, the factory-quoted value of which is known to be incorrect (Weir, 1970). No known gravity bases were available for most of the survey, so that calibration checks could not be easily performed in the field. However, the following checks were performed:

At the end of the 1968 field season a calibration check was run from Torbay Airport to the Seismic Vault of Memorial University, both places being gravity stations which are part of the Dominion Observatory network. This yielded a value for the instrument constant of 0.1016 mgal/division. Before the 1969 season this calibration run was repeated and the same value obtained. These were the only absolute check runs; however, the following two sets of data from the field work substantiate the idea that the constant did not change from July 1968 to May 1969, and from June to late July 1969.

The Lewisporte sub-base (9122) was run from Notre Dame Junction (9101) in July 1968 and again in May 1969, with no significant change in the gravity difference. Similarly, the run from Summerford (9125) to Indian Cove (9126) was undertaken in early June 1969, and again in July 1969. Again there was no significant change in the two sets of data. On the basis of these results it appears that the above value of the instrument constant (0.1016 mgal/div.) did not change from early July 1968 to late July 1969. A check run made in the fall of 1969 from Torbay Airport to the Seismic Vault again yielded a difference compatible with the above constant. However, this check consisted of a reading in the

vault, one at Torbay, and a final reading in the vault, i.e. a single run. The other check runs had been ABAB ... ABA, with at least four readings at B. From these arguments it appears that the instrument constant of 0.1016 mgal/div. is more reasonable that the value of the Dominion Observatory recalibration in 1966 of 0.10260 mgal/div. (Weir, 1970). The difference in these two values is of the order of 1% which would mean a maximum error of about + 0.20 mgal in any computed anomaly, since the maximum difference between a station and base is about 200 divisions on the instrument scale.

3.5.3 Combined Error. Summarizing the errors we have the following errors in a station anomaly:

(1) Observational error between ± 0.035 mgal and ± 0.05 mgal.

(2) Elevation error due to (i) density difference is less than ± 0.30 mgal for majority of stations, and (ii) elevation measurement is less than ± 0.4 mgal for more than 80% of the stations. Thus combining these the expected elevation error is less than ± 0.5 mgal for the majority of stations.

(3) Latitude error of approximately ± 0.08 mgal.

(4) Datum plane error of approximately - 0.14 mgal.

(5) Instrument scale error of approximately + 0.20 mgal.

Combining the random errors by standard error techniques (Topping, 1955) the probable random error is ± 0.5 mgal. The systematic error is + 0.06 mgal, thus the overall error for the survey is (+ 0.06 ± 0.5) mgal.

3.6 Separation of Regional and Residual Gravity

The Bouguer anomaly map (Map 1) reveals a regional trend due to deep-seated masses. Since the section of prime interest comprises the upper ten or fifteen kiolmeters of the crust, some method of separating deep-seated (large-wavelength) structures from the near surface (small-wavelength) structures must be found. The best methods of doing this employ Fourier or harmonic analysis. However, these techniques require equal station spacing on a regular grid. Since the station spacing in this survey was not uniform, these methods could only be used by placing a regular grid over the contoured anomaly map and interpolating between grid points. This would introduce errors of uncertain size, which would be propagated through the analysis with possible undesirable effects.

Elimination of these methods leaves a choice of visual smoothing or polynomial approximation. Since the total anomalies change fairly rapidly (i.e. small-wavelength components contribute prominently), visual smoothing would probably lead to errors. Thus a polynomial method was used. The technique was a least-squares fit using the Multiple Regression program in the IBM Scientific Programming Package. The program was run on an IBM 360/40 system.

The basic reasoning is as follows:

Let $g_i(x,y)$ = the observed gravity in milligals at the ith station with latitude y + 49°00'N and longitude x + 54°00'W (3.8)

where x,y are in minutes and fractions of a minute, and

$$G_i(x,y) = \sum_{k=0}^{n} \sum_{j=0}^{n=k} C_{kj} x^k y^j \qquad (3.9)$$

where n = order of polynomial;

G_i = computed anomaly from polynomial;

and where C_{kj} are to be determined by least squares fit.

Then the residual gravity anomaly,

$$R_i(x,y) = g_i(x,y) - G_i(x,y) \quad . \tag{3.10}$$

For a least squares fit,

$$\sum_{i=1}^{N} R_i^2(x,y) = \sum_{i=1}^{N} [g_i(x,y) - G_i(x,y)]^2 = \text{minimum} \tag{3.11}$$

where N = total number of data points.

The normal equations then become

$$\sum_{m=0}^{n} \sum_{\ell=0}^{n-m} C_{m\ell} \sum_{i=1}^{N} x^{m+k} y^{\ell+j} = \sum_{i=1}^{N} g_i x^k y^j \tag{3.12}$$

$$k = 0, 1, \ldots n$$

$$j = 0, 1, \ldots n-k$$

which can be written in matrix notation as

$$\left[\sum_{i=1}^{N} x^{k+m} y^{\ell+j}\right] [C_{m\ell}] = \left[\sum_{i=1}^{N} g_i x^k y^j\right] \tag{3.13}$$

for which the formal solution is

$$[C_{m\ell}] = \left[\sum_{i=1}^{N} x^{k+m} y^{\ell+j}\right]^{-1} \left[\sum_{i=1}^{N} g_i x^k y^j\right] \tag{3.14}$$

The program was modified so that the values of $R_i(x,y)$ and $G_i(x,y)$ were printed out. The solution was carried out for n = 1, 2, 3, 4, 5, and preliminary maps were drawn for n = 4 and n = 5. Profiles were drawn for all orders, and on the basis of these plus the contour maps for orders 4 and 5, it was decided to adopt the polynomial of order 5 as the one representing the regional. Order 5 was chosen, since it did not exhibit some of the undesirable fringe effects found on the order 4 map. Folded maps 2 and 3 show the regional and residual anomalies using a fifth order polynomial. The implications of these maps will be discussed in Chapter 5.

CHAPTER 4

SURFACE GEOLOGY

The geology of the surveyed area is very complicated since it has undergone intense deformation during the Taconic and Acadian orogenies. The exposed rocks are Ordovician, Silurian and Devonian. The northern part of the area has been cut by a right-lateral transcurrent fault, the Luke's Arm Fault, extending from the northeastern part of New World Island to the western boundary of the survey (Fig. 1.1). To the north of this fault are altered green lavas and pillow lavas (Williams, 1963; Horne and Helwig, 1969) of uncertain age. Intruded into these volcanics are the diorite and gabbro of Exploits Island and the Twillingate granodiorite batholith of Early Ordovician age. The geology south of this fault is much more complicated and is best treated by considering the following sub-areas: (i) Bay of Exploits; (ii) New World Island and Dildo Run; (iii) Change Islands and Fogo.

4.1 Bay of Exploits

There are two prominent features in the Bay of Exploits. The first is the Long Island batholith exposed over 16 x 8 km of the central part of the Bay. The second prominent feature is the complex of diorite, gabbro and minor ultrabasic rocks near Lewisporte.

A second granitic body is found near Birchy Bay; however, its surface extent and relation to other bodies is not known. Patrick (1956) tentatively denotes it as Devonian, but Professor M. Kay of Columbia

University (personal conversation) states that this age is very tentative and that K-Ar dating would be unlikely to yield conclusive results. The remaining rocks in the Bay of Exploits are Ordovician and Silurian sediments cut by numerous small faults. These rocks have some interbedded minor volcanics.

4.2 New World Island and Dildo Run

Geologically, New World Island and Dildo Run is the most complicated part of the area surveyed, and has been divided into four zones by Williams (1963) and Kay (1967).

(1) The area north of the Luke's Arm fault, where the rocks are mainly volcanic, as stated earlier.

(2) The area between the Luke's Arm and Cobb's Arm faults, known as the "central belt". This belt includes approximately 100 m of green pillow lavas; however, the predominant rock types are red and grey Silurian conglomerates and some Ordovician greywacke, siltstone and argillite. The conglomerate may be more than 300 m thick in some places.

(3) The "southern belt", which is the area between the Cobb's Arm and Dildo faults. The Ordovician in this belt is represented by slates and limestones. Basic to intermediate lavas are found on the islands of the Dildo Run, where structural interpretations are complicated and sometimes impossible. The Silurian in the southern belt is comprised mainly of a coarse conglomerate which may be more than 700 m thick.

(4) The Port Albert Peninsula has only Silurian rocks, represented by a deformed conglomerate sequence overlain by sheared green amygdaloidal lavas, which are in turn overlain by sandstones.

Kay (1967) and Williams (1963) inferred from the structure in the Port Albert Peninsula area that there might be a regionally significant fault between the Dildo Run and Port Albert Peninsula. Several smaller faults are found on New World Island in conjunction with either the Luke's Arm or Cobb's Arm faults. Several folds are found in the area, but the rocks involved are of comparable density, so that little, if any, variation in gravity can be expected.

4.3 Change Islands and Fogo Island

The most prominent feature of this area is the Fogo Island granodiorite batholith, exposed on more than half the island. Another prominent intrusion on Fogo is the diorite-gabbro complex near Tilting. Further, a basic intrusion is found around Seldom on the south end of Fogo. On the western side of the island the granite is overlain by sediments, which are also found near the town of Fogo. Change Islands are composed of the same sedimentary rock as on Fogo, with volcanics also present. Eastler (1969) suggests that the Change Islands beds continue along strike to the Port Albert sequence in one direction, and to Fogo in the other. He proposed that the Dildo fault meets the Luke's Arm fault to the north of Change Islands.

4.4 Rock Densities

The pertinent geological maps only yield a limited amount of information, so that the depth of various bodies cannot, in all cases, be estimated from surface geological features. However, if the densities of the main rock groups are known, one can construct models for which the

gravity anomaly may be computed. Thus a determination of rock density on the surface provides important information that can be applied to the interpretation of subsurface structures. In this survey, 223 rocks were collected and their density determined.

4.4.1 Density Measurement. The rock densities were measured by two standard procedures. The first consisted of weighing the rock in air, then coating it with liquid plastic and reweighing in air, then weighing the coated rock in water. The density of the liquid plastic was found to 1% by weighing a metal ring in air and water, then applying several coats of liquid plastic and weighing the coated ring in air and water again. The "coated" density method described here is accurate to 1% for samples exceeding 200 gm in air. The error is due to the error in the balance of ± 0.5 gm when the rock is placed on the pan. If the rock was suspended in a holder from the centre of the pan this error is 0.2 gm. The maximum error one can expect for a rock weighing less than 100 gm in air is 1.5%. There are only 15 samples out of a total of 223 in this category. The density of water was taken to be 1.000 gm/cm^3. Tables[1] indicate that for a temperature range 15^oC - 25^oC this is in error by 0.1% to 0.3% which is small compared to the overall error of about 1% from weighing.

After using this method for 84 samples collected in 1968, it was decided to see if the coated and uncoated densities were the same. Ten randomly selected rocks were allowed to soak in water for 3 months after being weighed in air. A t-test indicated that there was no significant change in density from the "coated" density for the same samples.

[1]Handbook of Physics & Chemistry, 44th edition, Chemical Rubber Company.

The samples collected in 1969 were only coated in the case of relatively porous rocks. The density of an uncoated rock was determined by weighing in air and in water. This method was accurate to 1% or better for rocks whose weight in air exceeded 100 gm.

4.4.2 Correlation. To facilitate model studies it was convenient to group the rocks into 13 blocks determined by the geological criteria discussed in Sections 4.1 - 4.3. For each of these blocks a mean density and standard deviation was determined. Table 4.1 gives the location, main rock type and relevant density information for each block. The table shows the following easily discernible features:

(1) The granite bodies (Blocks 1, 2, 6, 8) have densities falling in a narrow range close to that used for the Bouguer correction 2.67 gm/cm^3.

(2) The diorite dyke system near Lewisporte has a high density (2.79 gm/cm^3).

(3) The blocks (3, 4) north of the Luke's Arm fault have a high density contrast of almost 0.10 gm/cm^3 with the adjacent blocks.

(4) The blocks (7, 11, 12) composed mainly of sediments have densities near that of granite, i.e. higher than for typical sediments. Since these are deformed Ordovician and Silurian sediments, some increase from typical densities for sediments was expected.

The correlation between these results and the gravity anomalies will be discussed in Chapter 5.

TABLE 4.1

DENSITY INFORMATION

Block No.	Location and main rock types[1]	No. of Samples	Mean Density[2] gm/cm^3
1	Bay of Exploits, Granodiorite	8	2.68 ± 0.03
2	Twillingate, Granite	10	2.66 ± 0.02
3	North of Luke's Arm fault and West of Twillingate, Moreton's Hr., volcanics with small granitic intrusions	21	2.79 ± 0.11
4	North of Luke's Arm fault and East of Twillingate, volcanics	3	2.79 ± 0.10
5	Lewisporte area, sediments with diorite intrusions	73	2.79 ± 0.11
6	Birchy Bay, granite	8	2.66 ± 0.07
7	Port Albert Peninsula, Silurian sediments and volcanics	6	2.69 ± 0.09
8	Fogo, granite	3	2.67 ± 0.04
9	Fogo, diorite	4	2.80 ± 0.09
10	Botwood, Ordovician sediments	11	2.77 ± 0.12
11	Southern Belt, New World Island, sediments and minor volcanics	25	2.73 ± 0.13
12	Central Belt, New World Island, Ordovician sediments with minor volcanics	46	2.70 ± 0.08
13	Gayside, diorite	5	2.95 ± 0.13
Total		223	2.75

[1]From geological publications.

[2]Errors quoted are standard deviations.

(See Fig. 1.1 GENERAL GEOLOGY at end of document.)

CHAPTER 5

INTERPRETATION

Three gravity maps of the area have been drawn using the observed data (Appendix 1). The first (Map 1, in pocket) shows the anomalies calculated from equation (3.6), the second (Map 2) shows the regional anomalies, i.e. the values of $G(x,y)$ for $n = 5$ and the third (Map 3) shows the residuals $R(x,y)$ for $n = 5$ in Section (3.5).

5.1 Visual Interpretation

The total anomaly map (Map 1) shows several features which obviously correlate with surface geology (Chapter 4). This correlation is more obvious from a comparison of the surface geology with Map 3 where the effects of deep-seated structures have been removed. The maps can best be analyzed by considering the following features:

5.1.1 North of Luke's Arm Fault (Fig. 1.1). The linear features of the total anomaly pattern and the residual anomalies suggest a very sharp discontinuity in density (Fig. 4.1) across the geological feature known as the Luke's Arm Fault. This fault has long been known as one of the most important structural features of the area (Heyl, 1936; Horne and Helwig, 1969). The gravity maps suggest that this fault runs from the northeastern part of the survey area, between Change Islands and New World Island, across New World Island and the Bay of Exploits to the western boundary of the survey. Horne and Helwig offer geological evidence for continuing its trace westwards.

The steep gravity gradient across the fault strongly suggests that the fault has a high-angle with a sharp discontinuity. This hypothesis of a density discontinuity appears to be borne out from the sample densities (Table 4.1, Fig. 4.1) which show a mean value of 2.79 gm/cm^3 north of the fault, based on 24 samples; densities of 2.68 gm/cm^3, based on 8 samples in the Bay of Exploits (Block 1); and 2.70 gm/cm^3, based on 46 samples (Block 12). Since the regional map shows no steep gradient across the fault, it may be concluded that the density contrast has died out at the depth represented by the regional maps. The angle of the fault could be calculated under certain rigid conditions, if the density contrast and the depth to the bottom of the fault were known (Garland, 1965).

5.1.2 Long Island Batholith. The Long Island granodiorite is associated with the gravity low in the Bay of Exploits. Heyl (1936) mapped the batholith on the islands of the bay and assigned to it an area of about 16 x 8 km^2 at the surface. However, the shape of the contours on the total residual maps suggests that the body is elongated to the northeast along the Luke's Arm fault. Heyl suggested that the batholith may extend underneath the bay, and the gravity evidence seems to substantiate this suggestion. Indeed the batholith may extend much further east than was expected on geological grounds.

The western boundary of the batholith cannot be as clearly inferred, since there is a scarcity of stations between the western boundary of the survey and the batholith. The two factors contributing to this were (i) the bad boat landing conditions on the Fortune Harbour Peninsula and (ii) the width of water in which no islands exist.

The regional map shows some warping of the contours in the central part of the gravity low. This indicates that the depth to the bottom of the batholith is greater than the depth represented by the regional map.

5.1.3 Twillingate Granite. The Twillingate granite is believed to be of early Ordovician age; hence, it was emplaced prior to the movement on the Luke's Arm Fault. This is shown by shear zone in the granite on North Trump Island. The residual gravity map shows a roughly elliptical shape for the granite; however, its exact dimensions cannot be ascertained since only a profile was run from one end of the island to the other. Few islands exist to the northeast and southwest of Twillingate, so the width is hard to estimate.

The regional map shows no deformation in this area, so it was concluded that the Twillingate granite is a relatively shallow feature. On the basis of sparse data, the residual map shows closure of the contours over Twillingate Island, indicating an elliptical shape with the major axis perpendicular to strike.

The residual map also shows two lows south of the Luke's Arm fault, opposite the Twillingate granite, which appear to be related to the granite at shallow depth. However, the amplitude and areal extent of these features are too small to permit drawing conclusions.

5.1.4 Lewisporte High. This gravity high is the major feature which appears on all three maps; thus it must extend to greater depth than is represented by the regional anomaly. Geological maps indicate a progression of sediments cut by diorite dykes. From the gravity maps a

likely conclusion is that the diorite spreads out at depth. The mean density for rock samples in block 5 is 2.70 gm/cm^3, with individual values as high as 3.10 gm/cm^3. Both the total and residual maps indicate the same general shape for the body. It is impossible to say from the gravity maps whether the granite adjacent to the body was intruded before or after the diorite.

5.1.5 Birchy Bay Granite. This structure also appears on all maps. However, its presence on the regional map is probably caused by a lack of stations to the southeast, thus over-weighting the stations involved in determining the polynomial. The residual map suggests that this granite may extend northeast under Chapel Island, and that the granite found in the Dildo Run could be related to this body.

5.1.6 Sediments. The residual map indicates that the areas composed principally of sediments show small residual anomalies (Blocks 10, 11, 12). Thus it may be concluded that these sediments have little effect on the anomaly field.

5.1.7 Fogo-Change Islands. On all three maps the Fogo-Change Islands area appears to be a distinct entity, separate from the remainder of the survey area. From the geological evidence this is not surprising, since the sediments of this area are thought to be a continuation of the Port Albert sequence (Eastler, 1969), while the granite is believed to be Devonian (Baird, 1958). Sheridan and Drake (1968) show the structure under Fogo as a granite layer about 5 km thick, underlain by a basic to ultrabasic layer of undetermined thickness. The regional map shows

changes as one passed from the northern to the southern part of Fogo Island. However, the polynomial analysis is not expected to be as good here as in the main part of the survey area, since there are fewer stations.

The major geological features of the area show up on both the residual and total anomaly maps. The major feature is the low associated with the Fogo granodiorite which covers more than half the island. Towards the eastern end of Fogo there appears to be a high which would be consistent with the diorite found near Tilting. Since there are only three stations in this area, an accurate determination of the shape and depth of this body could not be expected from the data. The high on the southern end of the island also conforms to the diorite found there, but again accurate outlining of the body cannot be expected.

5.1.8 Other Features. Several other minor features are evident, some of which can be explained on the basis of surface geology and some cannot be explained. The largest feature in the latter category is in the extreme southwest corner of the survey area. There is no obvious explanation based on the surface geology for the observed anomalies.

The small changes across the postulated Dildo fault (Kay, 1967) are not sufficient to delineate its position as accurately as the Luke's Arm Fault. Similarly, there are few stations near the Cobb's Arm Fault. Also the density contrast across this fault is small (Blocks 11 and 12). The high on Exploits Island cannot be interpreted as an absolute high, as no readings were available to the north of it. Hence, any model considering this feature will have to be regarded as very approximate.

As can be seen from the maps, the major contribution to the gravity field in the area comes not from the surface features, which account for a maximum of 15 mgal of the total field. This means that the major contribution comes from a layer or layers at a depth represented by the regional anomaly. This mass can only be estimated from model studies.

5.2 Model Study

An interpretation of the maps in terms of depth and areal extent of the bodies must be undertaken if the survey is to be meaningful in quantitative terms. For this a model study was undertaken, using the basic formulae of Talwani and Ewing for calculating the effect of bodies of varying shape (Appendix 2).

The IBM 360/40 computer was used and a program was written for use with the IBM computer and tested by calculating the gravitational effect of a buried sphere. The sphere was approximated by six hexagonal prisms. Using this method, it was found that the computer result was 15% larger than the expected anomaly from exact formulae. A second test arose on the basis of some data run in the model program. A layer of material with infinite extent should give an anomaly of $2\pi Gz(\Delta\rho)$ mgal where G is the gravitation constant, $\Delta\rho$ is the density contrast, and z is the thickness of the layer. If $\Delta\rho = 0.15$ gm/cm^3 and z = 5 km, this anomaly should be 31.5 mgal. However, the anomaly calculated by the program suggested a maximum just over 38 mgal. Hence, the error here is of the order of 20%. Since, in the program, the shape of the body is unknown, it was assumed that the error would also be of this order. Thus, since

the average anomaly is about 30 mgal, an r.m.s. error of 5-6 mgal was as good a fit as could be expected for the model.

5.2.1 Application of Model. The area was first divided into 13 blocks according to the density results (Fig. 4.1). The first model was applied to the Fogo-Change Islands complex. Here the geology is well known (Baird, 1958; Eastler, 1969), so it was possible to use three blocks in this model, as shown (Fig. 5.1).

From the model it was found that the anomalies were too high near the boundary of blocks 8 and 9 , so these boundaries were revised. The anomalies now agreed fairly well except near the eastern and southern boundaries of Fogo Island. Smaller blocks were then added, which accounted for most of the misfit. The final Fogo-Change Islands model (Fig. 5.2, map 4) had an r.m.s. misfit of 4.91 mgal. The areas for which the fit is worst are at the boundaries of blocks 8 and 9 where the cause of the misfit probably resides.

The model of Figure 5.2 appears to explain the Fogo data, as follows. The western part of Fogo and all of Change Islands is composed of a body of density contrast + 0.10 gm/cm^3 while the main part of Fogo is a granodiorite batholith of density contrast - 0.05 gm/cm^3. The granite cuts underneath the western block, as shown in Figure 5.2. The whole area is underlain by a block of density contrast 0.15 gm/cm^3, which extends from 5 km to 10 km depth. Near Tilting on eastern Fogo, there is a diorite body which may extend as deep as 3 km. However, its true extent cannot be estimated, since only three stations are located near it. A similar body must exist to the south of Fogo, since there is geological

Fig. 5.1 Initial Model Fogo – Change Is.

$\Delta\rho$ = Density contrast

Z = Depth (km)

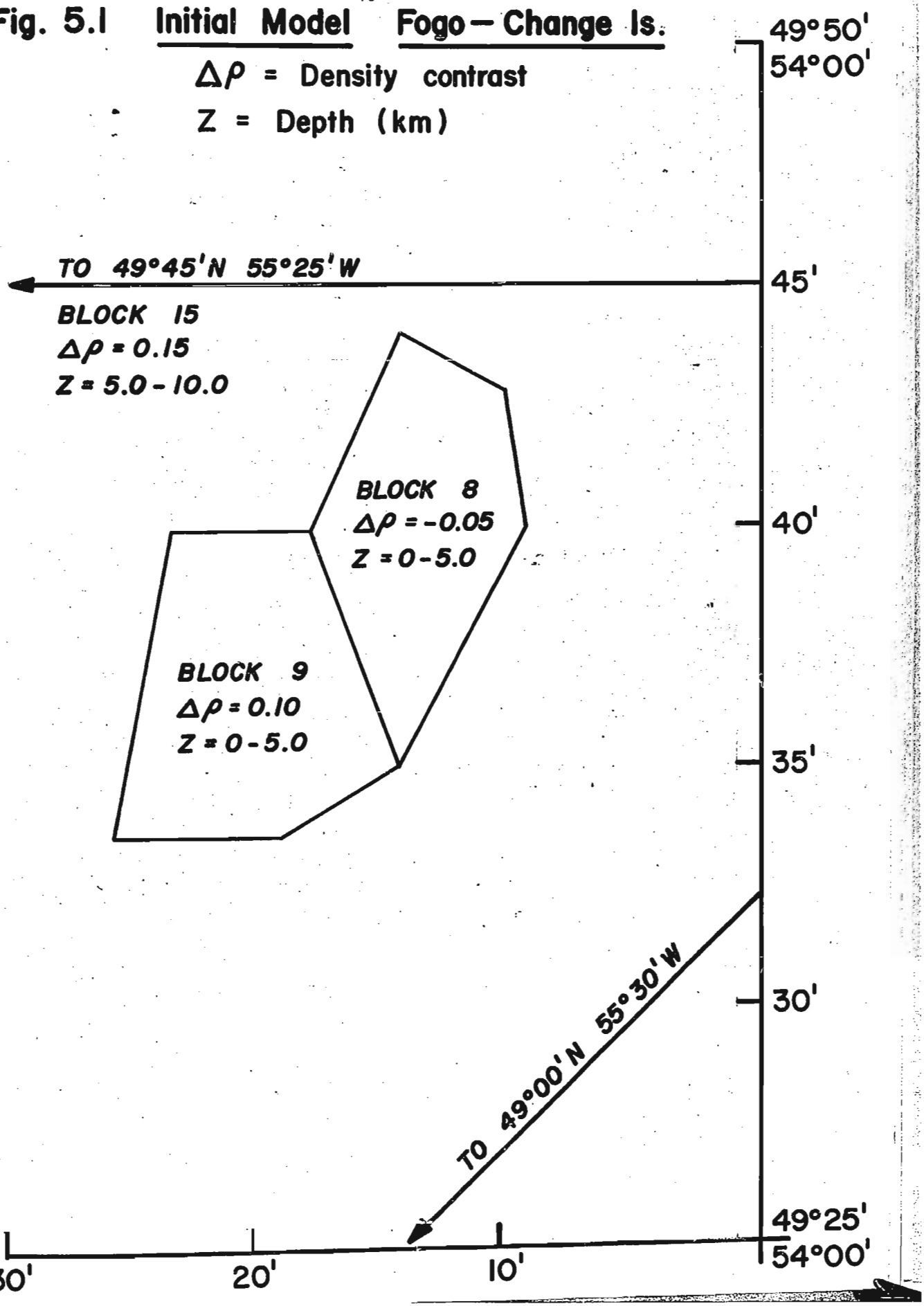

Fig. 5.2 Final Model Fogo — Change Is.

$\Delta\rho$ = Density contrast

Z = Depth (km)

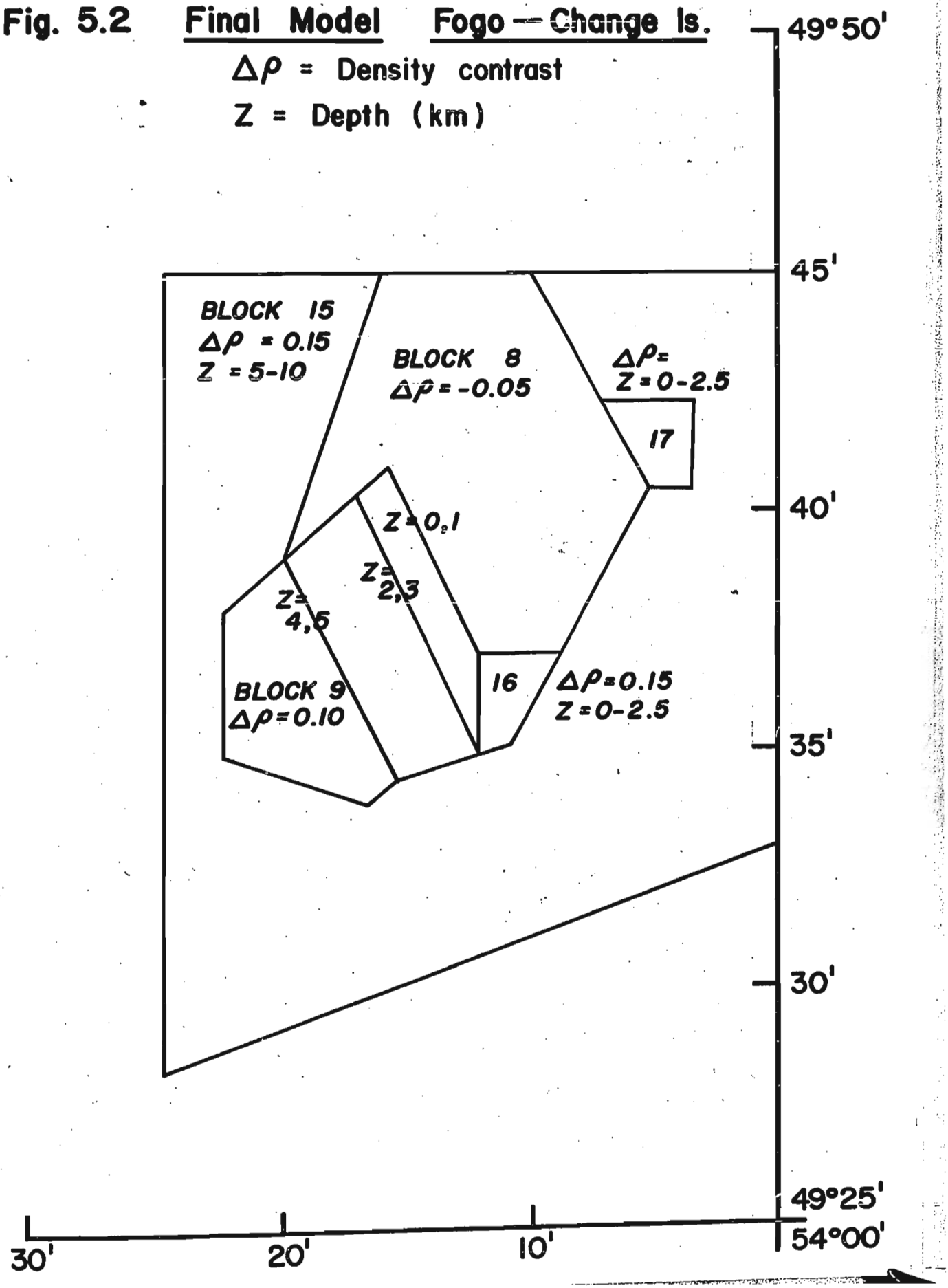

evidence for it on Fogo Island, and it must be at least 1 km thick to explain the anomalies found there.

The presence of the high-density layer below 5 km depth agrees with the results of Sheridan and Drake (1968) for Fogo Island. A small misfit in the core of Change Islands can probably by explained by a small shallow body of diorite, which is exposed over a small area at the surface (Eastler, 1969). This body was too small to incorporate in the model program.

5.2.2 Area West of Change Islands. Several features in this area have been discussed before. Map 4 is the contour map produced from the complete model (Fig. 5.3). The following conclusions are drawn on the basis of this model, for which the r.m.s. fit was 5.46 mgal based on 280 stations:

(1) The blocks (3, 4) north of Luke's Arm Fault extend without density change to about 5 km depth. The low calculated values for the five stations in the northwest corner of the map indicate that block 3 extends westward and northward beyond the survey area. The low calculated value on Exploits Island is consistent with the presence of a local near-surface, high-density body causing an additional anomaly of 10 mgal. The continuation of blocks 3 and 4 northward cannot be justified without more data.

(2) The Twillingate granite (Block 2) has small surficial extent, but may extend to 5 km depth. The shape and small size assumed for this body caused problems in the running of the model program, so that a better assessment of its dimensions could not be obtained.

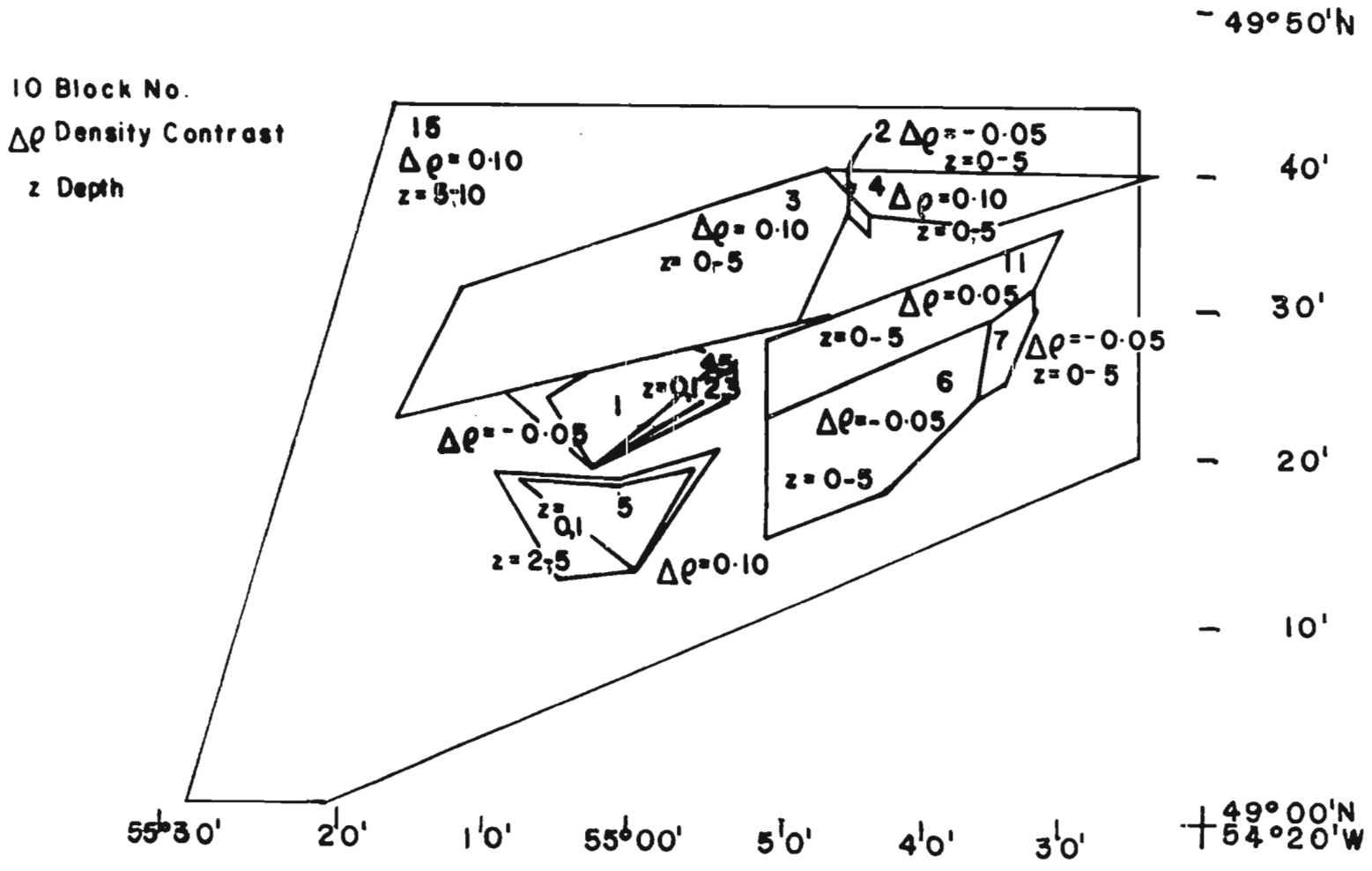

Fig. 5·3 Final Model - Bay of Exploits

(3) The Lewisporte high is caused by block 5, which may extend to 5 km or even greater depth. The exact shape of the block is again questionable. The maximum observed anomaly at the centre of the Lewisporte high is 32.0 mgal and the calculated value is 42.1 mgal. This misfit is larger than the 15% accountable from the program, but the flanking anomalies give a much better fit, so that it appears that the shape and/or depth of this body may have been wrongly chosen.

A readjustment of the depth would require that underlying layers be readjusted as well. Unfortunately, in the case of block 5, the corresponding uncertainty in the available geological information, and the dispersion in density values (Table 4.1) are exceptionally great.

(4) The Long Island batholith (Block 1) model works well. The assumed shape of the body produces an anomaly pattern (Map 4) very similar to that on Map 1. The minimum anomaly observed is 16.3 mgal and the calculated one 18.8 for a misfit of about 15%. The flanking anomalies tend to be a little low, so the sub-surface extent is not as great as shown in the model (Fig. 5.3).

(5) The Birchy Bay granite model (Block 6) produces a pattern (Map 4) that is too low. This indicates the model chosen is probably somewhat too large in areal extent, since it was based on incorporation of all granite observed on Comfort Cove peninsula, Chapel Island, Coal All Island, and near Birchy Bay.

(6) The Port Albert Peninsula anomalies can be explained on the basis of block 7. However, again it appears that the block assumed was too large, as the anomalies in the southwest part of this block are too large.

(7) The sediments appear to be a factor only in block 11, the southern block of New World Island. The model of 5 km of sediment appears to work fairly well. However, the block is a melange of smaller blocks, so the results should not be construed to mean that the sediments in all parts of the area extend to 5 km. Indeed, the other sedimentary blocks (10, 12) are not needed to explain the observed gravity values in their vicinity.

(8) Only one block remains to be discussed. This is block 15, underlying all others. At first a density contrast of + 0.15 gm/cm^3 was used for the 5-10 km layers, as in the Fogo model. However, this was found to cause anomalies too large by 50% for most of the area. Changing this to + 0.10 gm/cm^3, a much better fit was obtained. If the model of a layer between 5 and 10 km depth is correct, then this density contrast must be the best one. However, if the layer has thinned - the case of Block 15 - then the higher density contrast may be used. This layer in either case will explain the largest part of any anomaly.

The behaviour of the + 0.10 gm/cm^3 layer has not been remodelled. As mentioned earlier the layer possibly upwarps or thins under the Lewisporte high. There appears to be no necessity for extending the density contrast across the Luke's Arm fault to a depth greater than 5 km. This is not, however, all-conclusive evidence that the fault extends only to 5 km depth.

The gravity anomalies in the southwestern part of the survey area can be explained by truncating the block 15 layer as was done in the model. Thus the question of the continuation of this layer beyond the survey area is highly speculative. If this layer is the one proposed by

Sheridan and Drake (1968), why is there such a marked discontinuity of density at Change Islands between the Fogo model and the general model for the rest of the area? This question cannot be answered by the present survey.

The overall results of the model study give a map (Map 4) which is in good agreement with the observed anomalies (Map 1). On both of these maps the major features, such as the Luke's Arm Fault, the Long Island Batholith, the Lewisporte high and the Fogo-Change Islands complex have the same basic shape and magnitude. The above feature-by-feature discussion only illustrates the minor differences between the two maps and some of the difficulties in modelling the blocks.

The model work helps explain two important new features which could not be interpreted from a cursory glance at the geological maps or from the observed anomalies (Map 1). These features are (i) the decrease in gravity values as one proceeds up-river in the Exploits valley; (ii) the sharp change in gravity values near Change Islands. The model study has also shown that the major part of the anomalies cannot be explained solely by features which manifest themselves at the surface, but by a sub-surface structure.

CHAPTER 6

SUMMARY AND CONCLUSIONS

6.1 Summary

A gravity survey of Eastern Notre Dame Bay, Newfoundland, was undertaken, using a mean station spacing of 2.5 km. Gravity readings and elevations were taken at 308 stations. Nine gravity sub-bases were established. Rock samples were collected from 223 sites. On the basis of this data the following conclusions were drawn:

(1) The Bouguer anomalies are accurate to (+ 0.06 ± 0.5) mgal for over 80% of the stations.

(2) The geological setting, when coupled with the rock densities, leads to a division of the survey area into 13 major surface blocks.

(3) An analysis of the gravity data shows that there is a southwest-northeast regional trend in anomalies which can be removed by a polynomial of order 5.

(4) Model work shows that the gravity field can be explained, with an r.m.s. error of less than 6 mgal, by density changes in the upper 10 km of the crust. These models also reveal a major crustal discontinuity in the vicinity of Change Islands at a depth between 5 and 10 km. This feature, to which there appears to be no reference in previous publications, is also seen on an aeromagnetic map (Department of Mines and Resources, Map 4453G, 1969) which became available after the thesis was prepared.

(5) The closed highs and lows on the Bouguer anomaly map are due to diorite/gabbro and granite, respectively.

(6) The sediments in the area have little or no effect on the gravity field, thus it is difficult to ascribe exact vertical dimensions to them.

(7) The Luke's Arm Fault is the major structural feature in the northern part of the survey area. Its trace appears to extend out to sea to the northeast of the survey area.

6.2 Conclusions and Suggestions for Further Work

The survey does not answer some of the pertinent questions raised initially about the origin of the area. The finding of the higher density layer at depth 5 - 10 km is consistent with Dewey's (1969) hypothesis about the area. In the Fogo area it agrees with the conclusions of Sheridan and Drake (1968). However, the discontinuity at Change Islands requires further investigation by seismic and magnetic means before it can be accepted as a major structural discontinuity.

The behaviour of the layer at depth 5 - 10 km must also be investigated by seismic means in the southern part of the area since the gravity results are inconclusive.

The whole area seaward, i.e. north and east of the present survey, should be investigated before any all-inclusive hypothesis about the seaward extension of the Appalachians can be considered to be verified.

APPENDIX 1A

PRINCIPAL FACTS FOR GRAVITY STATIONS

Station No.	Location				Absolute Gravity cm/sec^2	Bouguer Anomaly (mgal)	Elevation (m)	Error Class
	Lat. N		Long. W					
	o	'	o	'				
11500	49	1.77	55	27.2	980.9947	7.2	23.1	4
11501	49	3.01	55	26.4	980.9999	17.6	59.0	4
11502	49	4.30	55	25.9	980.9883	4.9	63.2	4
11503	49	5.30	55	25.1	980.9980	6.5	29.5	4
11504	49	6.29	55	23.7	981.0021	7.8	22.9	4
11505	49	6.77	55	22.0	981.0080	10.3	9.5	4
11506	49	7.95	55	21.9	981.0089	9.2	8.1	4
11507	49	9.03	55	20.7	981.0110	10.1	9.8	4
11508	49	9.18	55	22.0	981.0104	9.7	12.4	4
11509	49	9.78	55	23.5	981.0138	10.8	5.1	4
11510	49	10.75	55	22.2	981.0153	11.7	9.3	4
11511	49	11.31	55	21.0	981.0160	11.7	10.4	4
11512	49	12.41	55	20.3	981.0208	15.1	11.0	4
11513	49	13.32	55	19.1	981.0266	18.7	7.1	4
11514	49	14.02	55	17.4	981.0285	21.5	16.8	3

APPENDIX 1A, Continued

Station No.	Location				Absolute Gravity cm/sec^2	Bouguer Anomaly (mgal)	Elevation (m)	Error Class
	Lat. N		Long. W					
	o	'	o	'				
11515	49	14.82	55	16.7	981.0322	22.5	9.0	3
11516	49	15.45	55	16.9	981.0354	24.5	8.3	3
11517	49	16.86	55	16.2	981.0276	24.7	58.9	3
11518	49	18.12	55	16.1	981.0312	25.3	53.8	3
11519	49	19.33	55	15.7	981.0322	32.2	59.1	3
11520	49	20.48	55	16.0	981.0439	26.6	13.0	3
11521	49	21.77	55	15.7	981.0446	27.8	25.4	3
11522	49	22.74	55	15.5	981.0500	28.5	9.3	3
11523	49	23.71	55	15.5	981.0498	32.3	36.7	3
11524	49	24.38	55	13.5	981.0533	30.2	13.4	3
11525	49	25.38	55	14.0	981.0478	29.7	46.8	3
11526	49	26.41	55	14.3	981.0498	30.1	46.0	3
11527	49	27.43	55	15.2	981.0496	32.3	66.2	3
11528	49	28.60	55	16.2	981.0539	33.1	56.9	3
11529	49	29.37	55	17.0	981.0642	34.9	19.8	3

APPENDIX 1A, Continued

Station No.	Location				Absolute Gravity cm/sec^2	Bouguer Anomaly (mgal)	Elevation (m)	Error Class
	Lat. N		Long. W					
	o	'	o	'				
11530	49	30.27	55	15.6	981.0716	43.1	30.7	3
11531	49	30.64	55	14.6	981.0789	45.2	6.6	1
11532	49	30.08	55	14.0	981.0762	43.1	5.9	1
11533	49	7.09	55	21.9	981.0087	10.0	6.5	1
11534	49	7.59	55	20.3	981.0099	11.1	9.6	1
11535	49	6.40	55	19.6	981.0093	12.0	8.0	1
11536	49	5.67	55	19.2	981.0100	12.8	3.0	1
11537	49	8.79	55	4.6	981.0000	14.7	87.6	3
11538	49	9.93	55	3.9	981.0117	17.7	51.6	3
11539	49	11.09	55	3.8	981.0184	20.1	38.8	3
11540	49	14.22	55	3.7	981.0346	25.5	7.9	3
11541	49	15.44	55	2.3	981.0391	29.6	14.9	3
11542	49	16.62	55	1.9	981.0438	33.5	20.1	3
11543	49	17.72	55	2.0	981.0471	32.0	4.1	3
11544	49	18.88	55	2.3	981.0472	30.4	3.5	1

APPENDIX 1A, Continued

Station No.	Location				Absolute Gravity cm/sec^2	Bouguer Anomaly (mgal)	Elevation (m)	Error Class
	Lat. N		Long. W					
	o	'	o	'				
11545	49	15.42	55	4.2	981.0392	30.2	17.2	3
11546	49	16.16	55	5.7	981.0393	28.8	15.4	3
11547	49	15.64	55	7.6	981.0265	24.9	56.5	3
11548	49	15.22	55	9.5	981.0330	22.8	9.5	3
11549	49	14.84	55	10.5	981.0289	20.7	17.0	3
11550	49	13.81	55	11.8	981.0218	21.5	49.8	3
11551	49	13.13	55	13.6	981.0168	19.6	59.8	3
11552	49	12.54	55	15.4	981.0148	19.6	65.5	3
11553	49	11.69	55	16.8	981.0229	16.6	3.1	3
11554	49	12.61	55	17.8	981.0225	14.8	3.0	1
11555	49	16.72	55	5.6	981.0427	29.7	6.8	1
11556	49	17.07	55	5.9	981.0449	30.7	3.2	1
11557	49	15.48	55	11.3	981.0343	23.0	6.0	1
11558	49	19.51	55	3.7	981.0479	30.4	5.0	3
11559	49	20.34	55	4.4	981.0459	29.0	14.3	3

APPENDIX 1A, Continued

Station No.	Location				Absolute Gravity cm/sec^2	Bouguer Anomaly (mgal)	Elevation (m)	Error Class
	Lat. N		Long. W					
	o	'	o	'				
11560	49	21.27	55	4.8	981.0452	24.8	3.7	1
11561	49	13.99	55	2.1	981.0354	26.1	4.6	3
11562	49	14.98	55	1.0	981.0384	28.9	11.3	3
11563	49	15.78	54	59.8	981.0411	29.7	7.6	3
11564	49	17.01	54	59.5	981.0441	31.7	11.7	3
11565	49	17.45	54	58.2	981.0409	31.5	30.7	3
11566	49	17.21	54	56.2	981.0418	28.8	6.6	1
11567	49	18.38	54	56.3	981.0421	26.6	10.7	3
11568	49	16.95	54	54.6	981.0382	27.2	18.7	4
11569	49	17.76	54	53.4	981.0373	23.0	8.0	4
11570	49	19.25	54	52.8	981.0387	23.4	14.0	4
11571	49	20.41	54	52.1	981.0428	24.2	6.1	4
11572	49	21.84	54	51.9	981.0456	24.9	6.5	4
11573	49	23.14	54	52.0	981.0457	26.8	25.2	4
11574	49	23.94	54	51.7	981.0516	26.9	1.8	4

APPENDIX 1A, Continued

Station No.	Location				Absolute Gravity cm/sec^2	Bouguer Anomaly (mgal)	Elevation (m)	Error Class
	Lat. N		Long. W					
	o	'	o	'				
11575	49	23.48	54	51.1	981.0507	26.9	3.0	1
11576	49	24.34	54	51.6	981.0517	26.6	2.8	1
11577	49	15.00	55	12.1	981.0371	25.6	1.6	1
11578	49	17.30	55	12.0	981.0411	26.2	1.5	1
11579	49	18.55	55	12.2	981.0429	26.1	1.2	1
11580	49	16.71	55	10.5	981.0399	25.7	1.0	1
11581	49	17.78	55	9.0	981.0439	28.3	1.6	1
11582	49	18.55	55	7.8	981.0472	30.2	.7	1
11583	49	19.55	55	12.2	981.0441	25.7	.9	1
11584	49	20.89	55	11.1	981.0445	25.2	.9	1
11585	49	20.68	55	9.4	981.0492	29.1	1.0	1
11586	49	19.57	55	8.9	981.0474	29.0	0.9	1
11587	49	16.63	54	52.7	981.0264	28.4	82.6	3
11588	49	16.23	54	51.0	981.0442	31.3	3.4	3
11589	49	16.86	54	49.8	981.0389	26.2	9.2	3

APPENDIX 1A, Continued

Station No.	Location				Absolute Gravity cm/sec^2	Bouguer Anomaly (mgal)	Elevation (m)	Error Class
	Lat. N		Long. W					
	o	'	o	'				
11590	49	17.77	54	48.5	981.0351	20.4	6.2	3
11591	49	18.21	54	46.5	981.0315	19.8	24.4	3
11592	49	19.15	54	45.4	981.0350	18.9	9.1	3
11593	49	20.22	54	44.8	981.0360	18.2	8.9	3
11594	49	21.28	54	44.3	981.0368	19.1	17.5	3
11595	49	21.97	54	42.5	981.0392	19.4	12.0	3
11596	49	23.00	54	41.3	981.0413	19.1	7.1	3
11597	49	24.00	54	40.3	981.0440	20.4	7.7	3
11598	49	25.30	54	39.7	981.0452	19.7	7.7	3
11599	49	26.46	54	39.8	981.0492	21.5	5.6	3
11600	49	7.81	55	11.6	981.0127	12.8	6.3	5
11601	49	7.27	55	13.7	981.0117	12.7	6.2	5
11602	49	6.78	55	14.7	981.0119	12.5	6.0	5
11603	49	6.12	55	16.0	981.0112	13.8	5.6	5
11604	49	5.70	55	16.9	981.0116	15.2	7.9	1

APPENDIX 1A, Continued

Station No.	Location		Absolute Gravity cm/sec^2	Bouguer Anomaly (mgal)	Elevation (m)	Error Class
	Lat. N	Long. W				
	o '	o '				
11605	49 27.60	54 39.8	981.0516	23.5	12.1	3
11606	49 28.08	54 41.1	981.0508	23.7	21.0	3
11607	49 27.83	54 43.2	981.0533	24.6	10.6	3
11608	49 28.05	54 45.1	981.0561	25.6	3.8	3
11609	49 28.84	54 45.8	981.0586	27.1	4.4	1
11610	49 29.77	54 46.8	981.0595	28.6	14.3	1
11611	49 29.05	54 46.8	981.0599	27.8	2.6	1
11612	49 29.39	54 48.2	981.0592	27.2	6.0	1
11613	49 29.39	54 50.0	981.0597	28.5	14.3	4
11614	49 30.41	54 51.7	981.0635	31.2	11.9	4
11615	49 30.62	54 52.1	981.0655	31.6	5.6	1
11616	49 30.81	54 52.0	981.0671	32.5	3.2	1
11617	49 30.68	54 51.3	981.0657	31.1	2.6	1
11618	49 19.86	54 45.9	981.0362	18.0	3.8	1
11619	49 20.95	54 46.0	981.0398	20.1	4.7	1

APPENDIX 1A, Continued

Station No.	Location				Absolute Gravity cm/sec^2	Bouguer Anomaly (mgal)	Elevation (m)	Error Class
	Lat. N		Long. W					
	o	'	o	'				
11620	49	31.17	54	46.6	981.0546	27.3	42.9	2
11621	49	32.21	54	46.8	981.0641	29.5	13.9	3
11622	49	32.53	54	48.5	981.0680	34.8	23.5	3
11623	49	33.23	54	49.6	981.0737	40.8	30.2	3
11624	49	33.51	54	51.4	981.0764	41.3	21.2	3
11625	49	33.00	54	52.7	981.0783	41.3	7.6	3
11626	49	34.14	54	51.9	981.0759	36.9	6.0	2
11627	49	34.72	54	53.1	981.0810	44.5	23.6	3
11628	49	33.81	54	53.7	981.0790	40.8	7.7	2
11629	49	34.14	54	54.0	981.0812	41.4	2.2	2
11630	49	34.72	54	52.3	981.0842	45.1	10.0	3
11631	49	34.90	54	50.4	981.0829	47.0	27.8	3
11632	49	35.32	54	48.9	981.0855	46.6	15.7	3
11633	49	35.29	54	48.5	981.0845	45.5	15.2	3
11634	49	32.11	54	44.9	981.0582	27.1	30.9	3

APPENDIX 1A, Continued

Station No.	Location				Absolute Gravity cm/sec^2	Bouguer Anomaly (mgal)	Elevation (m)	Error Class
	Lat. N		Long. W					
	o	'	o	'				
11635	49	32.75	54	43.5	981.0624	27.8	18.0	3
11636	49	33.56	54	42.7	981.0677	29.4	5.3	3
11637	49	34.70	54	41.6	981.0676	30.8	21.9	3
11638	49	35.36	54	40.4	981.0699	32.6	19.0	3
11639	49	36.27	54	39.8	981.0780	36.5	6.8	3
11640	49	37.43	54	39.5	981.0755	39.1	44.1	3
11641	49	37.86	54	37.9	981.0848	41.7	13.2	3
11642	49	38.36	54	37.1	981.0881	42.0	10.5	3
11643	49	38.46	54	36.7	981.0892	44.6	2.3	2
11644	49	35.43	54	38.1	981.0705	32.7	22.5	3
11645	49	36.19	54	36.0	981.0641	31.7	55.2	3
11646	49	37.05	54	34.4	981.0736	31.4	11.9	3
11647	49	37.81	54	34.6	981.0732	33.2	29.2	3
11648	49	37.71	54	36.2	981.0801	35.2	3.2	3
11649	49	38.07	54	36.3	981.0813	36.7	7.2	3

APPENDIX 1A, Continued

Station No.	Location				Absolute Gravity cm/sec^2	Bouguer Anomaly (mgal)	Elevation (m)	Error Class
	Lat. N		Long. W					
	o	'	o	'				
11650	49	38.24	54	35.5	981.0779	36.1	23.0	3
11651	49	36.84	54	33.7	981.0732	30.7	8.7	3
11652	49	35.36	54	41.0	981.0746	33.1	2.7	2
11653	49	34.44	54	42.3	981.0703	30.0	2.4	2
11654	49	33.09	54	43.9	981.0683	30.3	3.4	2
11655	49	33.09	54	45.0	981.0665	30.2	12.2	2
11656	49	26.33	54	37.8	981.0468	21.7	17.8	4
11657	49	26.22	54	36.3	981.0496	22.9	8.9	4
11658	49	26.74	54	34.8	981.0486	22.8	17.8	4
11659	49	27.38	54	32.8	981.0504	22.2	10.2	4
11660	49	28.46	54	31.8	981.0527	21.7	4.1	4
11661	49	29.77	54	31.2	981.0538	21.4	7.0	4
11662	49	30.89	54	30.4	981.0587	24.1	4.3	4
11663	49	31.97	54	30.8	981.0560	26.3	37.4	4
11664	49	32.52	54	31.3	981.0665	29.2	3.0	4

APPENDIX 1A, Continued

Station No.	Location				Absolute Gravity cm/sec^2	Bouguer Anomaly (mgal)	Elevation (m)	Error Class
	Lat. N		Long. W					
	o	'	o	'				
11665	49	32.74	54	31.7	981.0675	29.9	3.3	2
11666	49	37.21	54	42.3	981.0742	32.7	16.7	5
11667	49	38.05	54	43.9	981.0751	33.2	21.1	5
11668	49	38.82	54	45.6	981.0752	33.4	27.4	5
11669	49	39.35	54	46.5	981.0828	35.6	4.1	5
11670	49	40.17	54	47.3	981.0848	38.7	15.9	5
11671	49	40.79	54	48.2	981.0870	44.9	40.8	5
11672	49	39.69	54	44.9	981.0825	36.8	14.3	5
11673	49	40.14	54	43.6	981.0879	39.9	5.9	5
11674	49	37.76	54	45.5	981.0787	36.1	15.1	5
11675	49	37.00	54	45.0	981.0750	34.6	20.8	5
11676	49	36.72	54	43.9	981.0730	30.8	9.3	5
11677	49	28.72	54	52.3	981.0578	25.8	1.0	1
11678	49	28.38	54	50.4	981.0564	24.9	0.9	1
11679	49	29.00	54	48.5	981.0584	25.9	1.0	1

APPENDIX 1A, Continued

Station No.	Location		Absolute Gravity cm/sec^2	Bouguer Anomaly (mgal)	Elevation (m)	Error Class
	Lat. N	Long. W				
	o '	o '				
11680	49 27.79	54 48.9	981.0559	25.3	1.0	1
11681	49 25.98	54 48.6	981.0536	25.7	1.4	1
11682	49 25.46	54 48.5	981.0516	24.4	1.1	1
11683	49 25.49	54 50.2	981.0517	25.1	3.6	1
11684	49 26.49	54 50.6	981.0523	23.9	2.4	1
11685	49 27.76	54 47.1	981.0570	26.3	0.7	1
11686	49 26.19	54 46.8	981.0519	23.7	0.8	1
11687	49 25.16	54 46.0	981.0496	22.8	0.7	1
11688	49 24.63	54 46.8	981.0490	23.0	0.6	1
11689	49 23.43	54 46.0	981.0445	20.5	1.2	1
11690	49 23.53	54 47.9	981.0486	24.3	1.1	1
11691	49 24.36	54 48.8	981.0494	24.1	1.9	1
11692	49 25.15	54 51.7	981.0508	24.4	2.6	1
11693	49 24.36	54 52.7	981.0509	25.6	1.8	1
11694	49 25.17	54 55.5	981.0500	23.4	1.5	1

APPENDIX 1A, Continued

Station No.	Location		Absolute Gravity cm/sec^2	Bouguer Anomaly (mgal)	Elevation (m)	Error Class
	Lat. N	Long. W				
	o '	o '				
11695	49 27.10	54 55.6	981.0501	20.6	1.3	1
11696	49 27.44	54 52.5	981.0542	24.2	1.6	1
11697	49 23.12	54 53.8	981.0511	27.5	1.1	1
11698	49 21.89	54 54.7	981.0506	28.7	0.9	1
11699	49 20.64	54 54.1	981.0447	24.8	1.7	1
11700	49 21.34	54 58.0	981.0479	26.9	0.8	1
11701	49 22.49	54 56.7	981.0503	27.6	0.8	1
11702	49 23.82	54 55.9	981.0509	26.2	0.9	1
11703	49 28.97	54 53.5	981.0554	23.1	1.3	1
11704	49 29.05	54 55.2	981.0610	28.6	1.1	1
11705	49 30.44	54 56.9	981.0687	34.2	1.3	1
11706	49 31.83	54 58.2	981.0836	47.0	1.0	1
11707	49 33.44	54 58.3	981.0843	45.3	1.0	1
11708	49 31.00	55 4.3	981.0884	53.4	2.7	1
11709	49 29.70	55 6.1	981.0773	43.9	1.3	1

APPENDIX 1A, Continued

Station No.	Location		Absolute Gravity cm/sec^2	Bouguer Anomaly (mgal)	Elevation (m)	Error Class
	Lat. N	Long. W				
	o '	o '				
11710	49 25.34	54 58.6	981.0456	18.7	1.2	1
11711	49 24.60	54 59.8	981.0421	16.3	1.5	1
11712	49 23.02	55 00.5	981.0417	18.4	1.9	1
11713	49 21.41	54 59.7	981.0463	25.3	1.4	1
11714	49 21.17	55 1.4	981.0443	23.5	1.0	1
11715	49 23.35	55 6.8	981.0497	25.8	1.5	1
11716	49 22.74	55 7.6	981.0523	29.2	0.9	1
11717	49 23.76	55 8.1	981.0504	25.8	1.1	1
11718	49 24.65	55 7.7	981.0514	25.5	1.4	1
11719	49 26.06	55 6.2	981.0527	24.8	1.5	1
11720	49 24.81	55 3.3	981.0432	17.1	1.4	1
11721	49 24.46	55 1.4	981.0424	16.8	1.4	1
11722	49 28.00	54 56.2	981.0537	22.9	2.0	1
11723	49 26.96	54 57.8	981.0498	20.4	1.3	1
11724	49 26.60	54 59.2	981.0483	19.6	1.8	1

APPENDIX 1A, Continued

Station No.	Location				Absolute Gravity cm/sec^2	Bouguer Anomaly (mgal)	Elevation (m)	Error Class
	Lat. N		Long. W					
	o	'	o	'				
11725	49	26.89	55	00.8	981.0481	18.8	1.1	1
11726	49	25.35	55	1.4	981.0448	16.7	1.0	1
11727	49	26.02	55	1.6	981.0470	19.0	0.9	1
11728	49	26.79	55	4.1	981.0533	24.4	2.3	1
11729	49	27.24	55	4.7	981.0574	27.6	0.7	1
11730	49	28.36	55	3.3	981.0642	32.7	0.9	1
11731	49	29.11	55	4.8	981.0725	39.9	0.6	1
11732	49	28.50	55	2.3	981.0629	31.3	0.8	1
11733	49	27.88	55	1.3	981.0591	28.3	0.9	1
11734	49	27.57	55	0.3	981.0557	25.4	1.0	1
11735	49	35.36	54	42.4	981.0738	32.0	1.5	1
11736	49	34.70	54	43.2	981.0726	31.8	1.2	1
11737	49	34.08	54	44.8	981.0716	31.6	1.1	2
11738	49	34.38	54	46.0	981.0732	32.9	1.4	2
11739	49	35.28	54	46.6	981.0812	39.6	1.4	2

APPENDIX 1A, Continued

Station No.	Location				Absolute Gravity cm/sec^2	Bouguer Anomaly (mgal)	Elevation (m)	Error Class
	Lat. N		Long. W					
	o	'	o	'				
11740	49	34.44	54	46.9	981.0771	36.7	1.5	2
11741	49	24.17	54	44.9	981.0457	20.5	1.2	1
11742	49	23.54	54	43.0	981.0433	18.9	1.2	1
11743	49	25.14	54	42.3	981.0471	20.4	0.4	1
11744	49	26.26	54	41.8	981.0500	22.6	1.2	1
11745	49	27.12	54	40.7	981.0533	23.6	0.8	1
11746	49	27.77	54	37.8	981.0535	23.0	1.3	2
11747	49	28.88	54	36.8	981.0560	23.9	1.8	2
11748	49	29.77	54	35.8	981.0590	25.5	1.5	2
11749	49	30.94	54	34.4	981.0623	27.2	1.8	2
11750	49	32.10	54	33.5	981.0649	28.0	1.5	2
11751	49	31.56	54	36.4	981.0615	25.4	1.7	2
11752	49	31.00	54	38.4	981.0615	26.2	1.5	2
11753	49	29.68	54	38.4	981.0585	25.2	1.4	2
11754	49	28.72	54	38.7	981.0555	23.6	1.6	2

APPENDIX 1A, Continued

Station No.	Location				Absolute Gravity cm/sec^2	Bouguer Anomaly (mgal)	Elevation (m)	Error Class
	Lat. N		Long. W					
	o	'	o	'				
11755	49	28.67	54	40.1	981.0556	23.7	1.0	2
11756	49	29.81	54	41.5	981.0586	24.9	1.0	2
11757	49	28.88	54	42.5	981.0565	24.3	1.0	2
11758	49	29.03	54	44.4	981.0587	26.4	1.9	2
11759	49	29.94	54	43.2	981.0592	25.3	1.0	2
11760	49	30.75	54	43.8	981.0621	27.1	1.1	2
11761	49	31.69	54	43.3	981.0641	27.8	1.2	2
11762	49	31.07	54	42.2	981.0619	26.5	1.7	2
11763	49	31.50	54	40.1	981.0642	27.9	1.1	2
11764	49	32.23	54	41.5	981.0651	27.9	1.1	2
11765	49	32.56	54	39.1	981.0656	28.0	1.3	2
11766	49	32.75	54	37.4	981.0662	28.3	1.4	2
11767	49	36.17	54	33.2	981.0696	26.7	1.6	2
11768	49	34.75	54	33.6	981.0698	28.9	1.2	2
11769	49	33.53	54	35.7	981.0674	28.3	1.7	2

APPENDIX 1A, Continued

Station No.	Location		Absolute Gravity cm/sec^2	Bouguer Anomaly (mgal)	Elevation (m)	Error Class
	Lat. N	Long. W				
	o '	o '				
11770	49 37.39	54 32.3	981.0742	29.5	1.9	2
11771	49 37.87	54 31.8	981.0750	29.6	2.0	2
11772	49 39.04	54 34.3	981.0848	37.7	2.0	2
11773	49 38.15	54 33.2	981.0787	32.8	1.6	2
11774	49 40.30	54 24.4	981.0818	32.8	2.5	2
11775	49 38.50	54 24.1	981.0796	33.3	1.8	2
11776	49 36.94	54 25.4	981.0781	34.1	2.3	2
11777	49 36.14	54 25.4	981.0773	34.5	2.3	2
11778	49 34.30	54 24.8	981.0731	32.9	1.4	2
11779	49 33.73	54 29.5	981.0712	31.8	1.3	2
11780	49 43.45	54 16.9	981.0702	17.3	6.3	1
11781	49 43.02	54 16.1	981.0685	17.0	10.1	1
11782	49 42.09	54 15.5	981.0550	17.1	71.8	5
11783	49 41.14	54 14.3	981.0532	18.1	79.2	5
11784	49 40.00	54 13.5	981.0636	20.8	31.3	5

APPENDIX 1A, Continued

Station No.	Location				Absolute Gravity cm/sec^2	Bouguer Anomaly (mgal)	Elevation (m)	Error Class
	Lat. N		Long. W					
	o	'	o	'				
11785	49	38.93	54	13.4	981.0678	27.4	35.4	5
11786	49	38.00	54	12.5	981.0701	32.8	43.8	5
11787	49	36.77	54	10.9	981.0837	40.0	2.7	2
11788	49	36.33	54	11.7	981.0772	40.8	38.0	5
11789	49	35.95	54	13.1	981.0795	38.0	8.0	5
11790	49	35.62	54	14.6	981.0647	37.1	79.4	5
11791	49	35.21	54	16.3	981.0705	35.4	36.4	5
11792	49	34.37	54	16.5	981.0757	36.6	8.0	2
11793	49	40.66	54	11.7	981.0662	17.4	6.1	2
11794	49	41.80	54	11.3	981.0635	16.6	24.0	5
11795	49	43.08	54	11.5	981.0652	16.2	23.1	5
11796	49	43.48	54	10.5	981.0700	17.4	8.2	5
11797	49	43.40	54	9.1	981.0699	18.6	13.5	5
11798	49	43.08	54	7.2	981.0598	21.0	78.9	5
11799	49	42.59	54	5.5	981.0784	28.3	13.6	5

APPENDIX 1B

PRINCIPAL FACTS FOR GRAVITY BASES

Base	No.	Latitude	Longitude	Absolute gravity (cm/sec^2)	Sta. error (mgal)
		o '	o '		
Bishop's Falls	9001-64	49 01.00	55 28.7	980.99137	*
Notre Dame Jct.	9101-66	49 07.64	55 05.4	980.99921	**
Botwood	9121-68	49 08.60	55 20.5	981.00953	± 0.06
Lewisporte	9122-68	49 12.98	55 03.2	981.03083	± 0.04
Little Burnt Bay	9123-68	49 21.27	55 04.8	981.04517	± 0.01
Boyd's Cove	9124-68	49 27.25	54 39.2	981.05230	± 0.05
Summerford	9125-69	49 29.57	54 46.8	981.06058	± 0.02
Indian Cove	9126-69	49 35.81	54 41.4	981.07631	± 0.02
Twillingate Ferry	9127-69	49 35.82	54 42.1	981.07446	± 0.01
Cobb's Arm	9128-69	49 37.19	54 34.2	981.07518	± 0.04
Fogo	9129-69	49 42.93	54 17.55	981.07025	± 0.05

*Dominion Observatory Base.

**Established by Weir, 1966.

APPENDIX 2

MODEL PROGRAM

A computer program based on formulae given by Talwani and Ewing (1960) was used to compute anomalies due to assumed mass distribution.

Consider an irregularly-shaped body (Fig. A2.1). The gravitational attraction due to a lamina of thickness dz is given by

$$\Delta g = V dz \tag{A2.1}$$

where formally

$$V = k\rho \left[\oint d\psi - \oint z/(r^2 + z^2)^{\frac{1}{2}}\, d\psi\right] \tag{A2.2}$$

where r, z, ψ are cylindrical coordinates used to define the boundary of the lamina.

If polygons are used to represent the lamina, then

$$V = k\rho \sum_{i=1}^{n} \left[W \arccos \left\{ \frac{x_i}{r_i}\,\frac{x_{i+1}}{r_{i+1}} + \frac{y_i}{r_i}\,\frac{y_{i+1}}{r_{i+1}} \right\} - \arcsin \frac{zq_iS}{(P_i^2 + z^2)^{\frac{1}{2}}} + \arcsin \frac{zf_iS}{(P_i^2 + z^2)^{\frac{1}{2}}} \right] \tag{A2.3}$$

where x_i, y_i, z and x_{i+1}, y_{i+1}, z are coordinates of successive vertices of the polygon in the coordinate system in (A2.1).

$S = +1$ if P_i is positive $S = -1$ if ρ_i is negative

$W = +1$ if M_i is positive $S = -1$ if m_i is negative

$$P_i = \frac{y_i - y_{i+1}}{r_{i,i+1}} \cdot x_i - \frac{x_i - x_{i+1}}{r_{i,i+1}} \cdot y_i$$

$$q_i = \frac{x_i - x_{i+1}}{r_{i,i+1}} \cdot \frac{x_i}{r_i} + \frac{y_i - y_{i+1}}{r_{i,i+1}} \cdot \frac{y_i}{r_i}$$

$$f_i = \frac{x_i - x_{i+1}}{r_{i,i+1}} \cdot \frac{x_{i+1}}{r_{i+1}} + \frac{y_i - y_{i+1}}{r_{i,i+1}} \cdot \frac{y_{i+1}}{r_{i+1}}$$

$$m_i = \frac{y_i}{r_i} \cdot \frac{x_i}{r_{i+1}} - \frac{y_{i+1}}{r_{i+1}} \cdot \frac{x_i}{r_i}$$

$$r_i = + (x_i 2 + y_i^2)^{\frac{1}{2}}$$

$$r_{i+1} = + (x_{i+1}^2 + y_{i+1}^2)$$

$$r_{i,i+1} = + [(x_i - x_{i+1})^2 + (y_i - y_{i+1})^2] \quad .$$

The program solves (A2.3) for V for each lamina and then integrates over the depth as follows. Let V_1, V_2, V_3 represent V at depths z_1, z_2, z_3, then, using the following quadrature formula, we get

$$\int_{Z_1}^{Z_3} V dz = \frac{1}{6} \left[V_1 \frac{(z_1 - z_3)}{(z_1 - z_2)} (3z_2 - z_3 - 2z_1) \right. \tag{A2.4}$$

$$\left. + V_2 \frac{(z_1 - z_3)^3}{(z_2 - z_3)(z_2 - z_1)} + V_3 \frac{(z_1 - z_3)}{(z_3 - z_2)} (3z_2 - z_1 - 2z_3) \right].$$

By using successive sets of three points P, the integration can be carried over the body. Thus, the anomaly due to the body can be

calculated at a specified location. This procedure is repeated for all bodies in the model and the total anomaly at the station is obtained. The calculated anomaly is compared with the observed anomaly at that station. An r.m.s. error is calculated as follows:

$$\text{R.m.s.} = \sqrt{\frac{(\text{observed anomaly} - \text{calculated anomaly})^2}{\text{number of stations}}} \qquad \text{(A2.5)}$$

The model is adjusted by changing the shapes and densities of the blocks until the R.m.s. appears to be minimized.

The method was tested by calculating the anomaly due to a buried sphere. It was found that the answer obtained using the program was approximately 15% too high. Similar results were found for a large sheet of 5 kilometers thickness. Since most anomalies were of the order of 30 mgal, the model was accepted if the R.m.s. was $\sim$ 5 - 6 mgal.

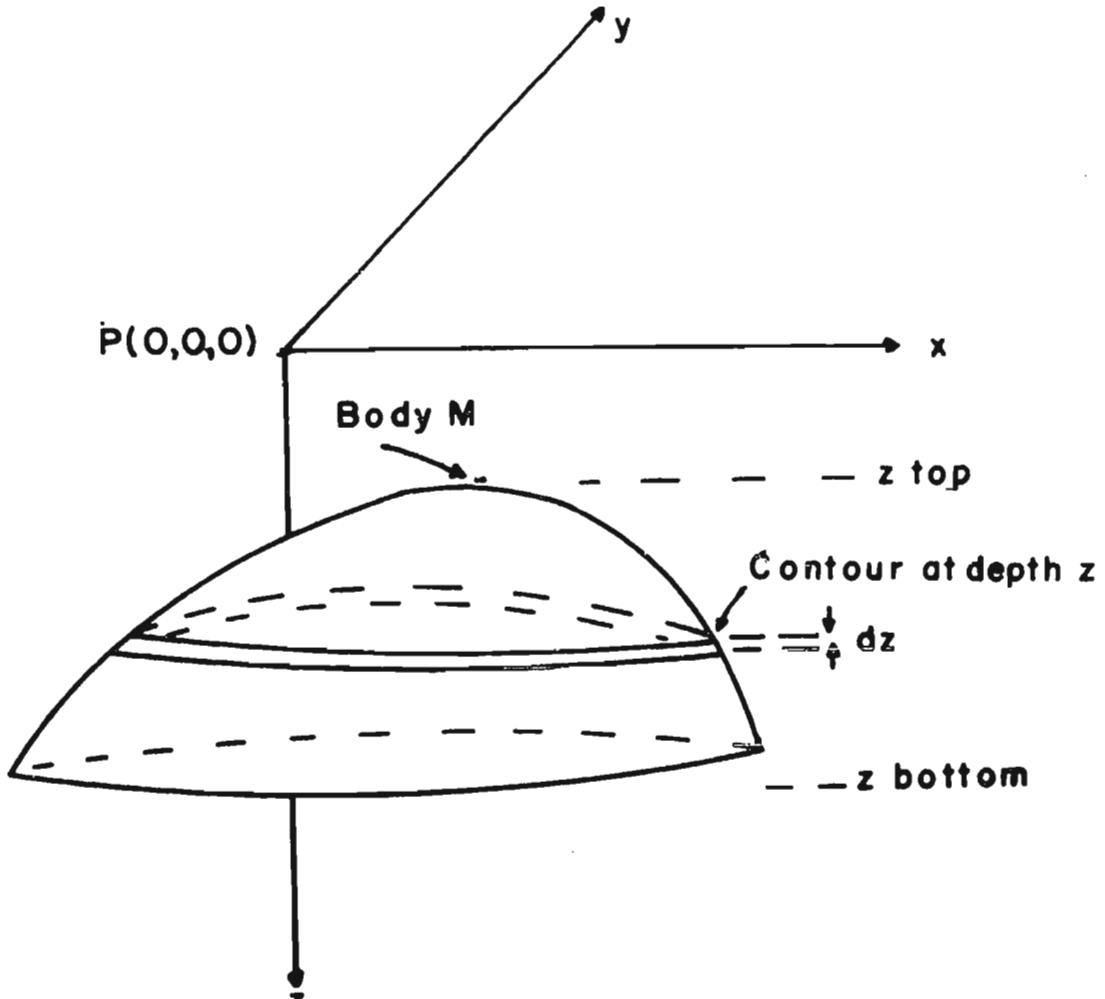

Fig. A2·1 Lamina Model used by Talwani and Ewing (1960)

ACKNOWLEDGEMENTS

The author wishes to acknowledge with thanks the following individuals and organizations without whose assistance this project could not have been undertaken:

Dr. S. W. Breckon, Head of the Department of Physics, for arranging for employment of field assistants and for the use of departmental equipment and facilities.

Dr. E. R. Deutsch, my supervisor, for the original idea for the survey and for many helpful hints during the course of my work.

Dr. H. Williams of the Department of Geology for numerous valuable discussions about the geology of the area and for the use of personal files and notes.

Dr. J. A. Wright, Department of Physics, for many useful suggestions about data treatment and analysis.

Messrs. D. F. Granter, R. P. Kennedy, and L. M. Smith for invaluable help as field assistants during 1968 and 1969.

Mr. H. Weir, Department of Physics, for numerous discussions and suggestions during all stages of the project, and for proof-reading the manuscript.

Mr. P. Gillard, Department of Physics, for assistance with the computer program for fitting polynomials.

Mr. S. C. Pande, Department of Physics, for assistance in determining sample densities.

Mr. R. Tucker, Department of Physics, for drafting the maps and figures.

Miss D. Janes, Department of Physics, for typing the thesis.

Drs. M. J. Innes and D. Nagy, Gravity Division, Earth Physics Branch, Department of Energy, Mines, and Resources, for information about previous gravity work in Newfoundland and for a copy of their model study computer program.

Dr. M. Talwani, Lamont-Doherty Geological Observatory, for providing a copy of his model study program.

National Research Council of Canada for providing the author with a postgraduate scholarship to undertake these studies.

National Research Council of Canada for providing funds for field expenses during the summer of 1968 and 1969 through grant NRC-A-1946 to Dr. E. R. Deutsch.

REFERENCES

Baird, D. M. (1958) Fogo Island map area, Newfoundland; Geol. Surv. Canada, Memoir 301, Ottawa, 43p.

Bullard, Sir Edward, Everett, J. E., and Smith, A. Gilbert (1965) The fit of the continents around the Atlantic, in A Symposium on Continental Drift; Phil. Trans. Roy. Soc. 1088.

Clark, J. D. (ed.) (1967) Appalachian Tectonics, Royal Society of Canada; Special Publication No. 10, Univ. Toronto Press, 140p.

Dewey, J. F. (1969) Evolution of the Appalachian/Caledonian Orogen; Nature 222, p. 124.

Eastler, J. E. (1969) Silurian geology of Change Islands and Eastern Notre Dame Bay, Nfld., p. 245 in North Atlantic - Geology and Continental Drift; Am. Assoc. Petrol. Geologists Memoir 12, M. Kay (ed.), Tulsa, Okla.

Ewing, G. N., Dainty, A. M., Blanchard, J. E., and Keen, M. J. (1966) Seismic studies on the eastern seaboard of Canada: The Appalachians System 1; Can. J. Earth Sci., 3, p. 89.

Fenwick, D. K. B., Keen, M. J., Keen, Charlotte, and Lambert, A. (1968) Geophysical studies on the continental margin northeast of Newfoundland; Can. J. Earth Sci., 5, p. 483.

Garland, G. D. (1965) The Earth's Shape and Gravity; Pergamon Press, Oxford, 183p.

Grant, F. S. (1957) A problem in the analysis of geophysical data; Geophysics 22, p. 309.

Grant, F. S. and West, G. F. (1965) Interpretation Theory in Applied Geophysics; McGraw-Hill, New York, 584p.

Hammer, S. (1939) Terrain corrections for gravimeter stations; Geophysics 4, p. 184.

Heyl, G. R. (1936) Geology and mineral deposits of the Bay of Exploits area, Newfoundland; Geological Section, Dept. of Natural Resources, St. John's, Nfld.

Horne, G. S. and Helwig, James (1969) Ordovician stratigraphy of Notre Dame Bay, Nfld., p. 388 in North Atlantic - Geology and Continental Drift; Am. Assoc. Petrol. Geologists Memoir 12, M. Kay (ed.), Tulsa, Okla.

Kay, M. (1967) Stratigraphy and structure of northeastern Newfoundland bearing on drift in the North Atlantic; Am. Assoc. Petrol. Geologists Bull., 51^1, p. 579.

Krumbein, W. C. (1959) Trend surface analysis of contour-type maps with irregular control point spacing; J. Geoph. Res., 64, p. 823.

Melchior, P. (1968) The Earth Tides; Pergamon Press, Oxford, 458p.

Nagy, D. (1964) The gravitational effect of three-dimensional bodies of arbitrary shape; Unpubl. Man., Gravity Division, Dept. of Mines and Tech. Surveys, Ottawa, 39p.

Patrick, T. O. H. (1956) Comfort Cove, Newfoundland; Geol. Surv. Canada Paper 55-31, Ottawa.

Sheridan, R. E. and Drake, C. L. (1968) Seaward extension of the Canadian Appalachians; Can. J. Earth Sci., 5, p. 337.

Simpson, S. M., Jr. (1954) Least square polynomial fitting to gravitational data and density plotting by digital computers; Geophysics 19, p. 255.

Talwani, M. and Ewing, M. (1960) Rapid computation of gravitational attraction of three dimensional bodies of arbitrary shape; Geophysics 25, p. 203.

Topping, J. (1955) Errors of Observation and their Treatment; Chapman and Hall, Ltd., London, 119p.

Weaver, D. F. (1967) A geological interpretation of the Bouguer anomaly field of Newfoundland; Publ. Dom. Obs. XXXV No. 5, Dept. of Energy, Mines, and Resources, Ottawa.

Wegener, A. (1966) The origin of continents and oceans; Engl. trans. by John Biram of 1921 version, Dover Publ. Inc., New York, 246p.

Weir, H. (1970) A gravity profile across Newfoundland; Memorial Univ. of Nfld. (M.Sc. thesis in preparation).

Williams, H. (1963) Twillingate map area, Nfld.; Geol. Surv. Canada Paper 63-36, Ottawa, 30p.

_____ (1964) The Appalachians in Northeastern Newfoundland - A two-sided symmetry; Amer. Jour. Sci., 267, p. 1137.

_____ (1969) Precarboniferous development of Newfoundland Appalachians, p. 32 in North Atlantic - Geology and Continental Drift; Am. Assoc. Petrol. Geologists Memoir 12, M. Kay (ed.), Tulsa, Okla.

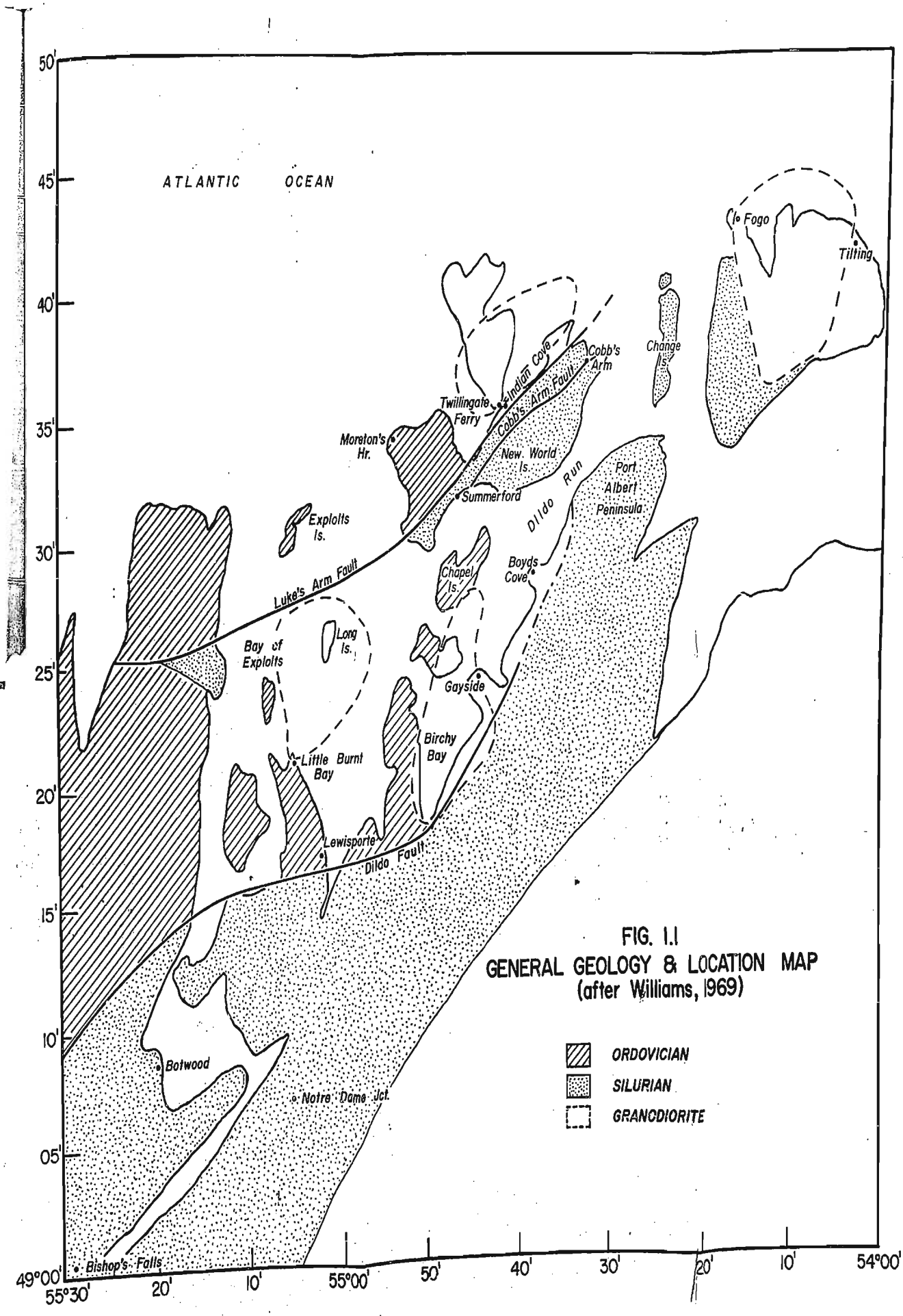

FIG. 1.1
GENERAL GEOLOGY & LOCATION MAP
(after Williams, 1969)

ORDOVICIAN
SILURIAN
GRANODIORITE

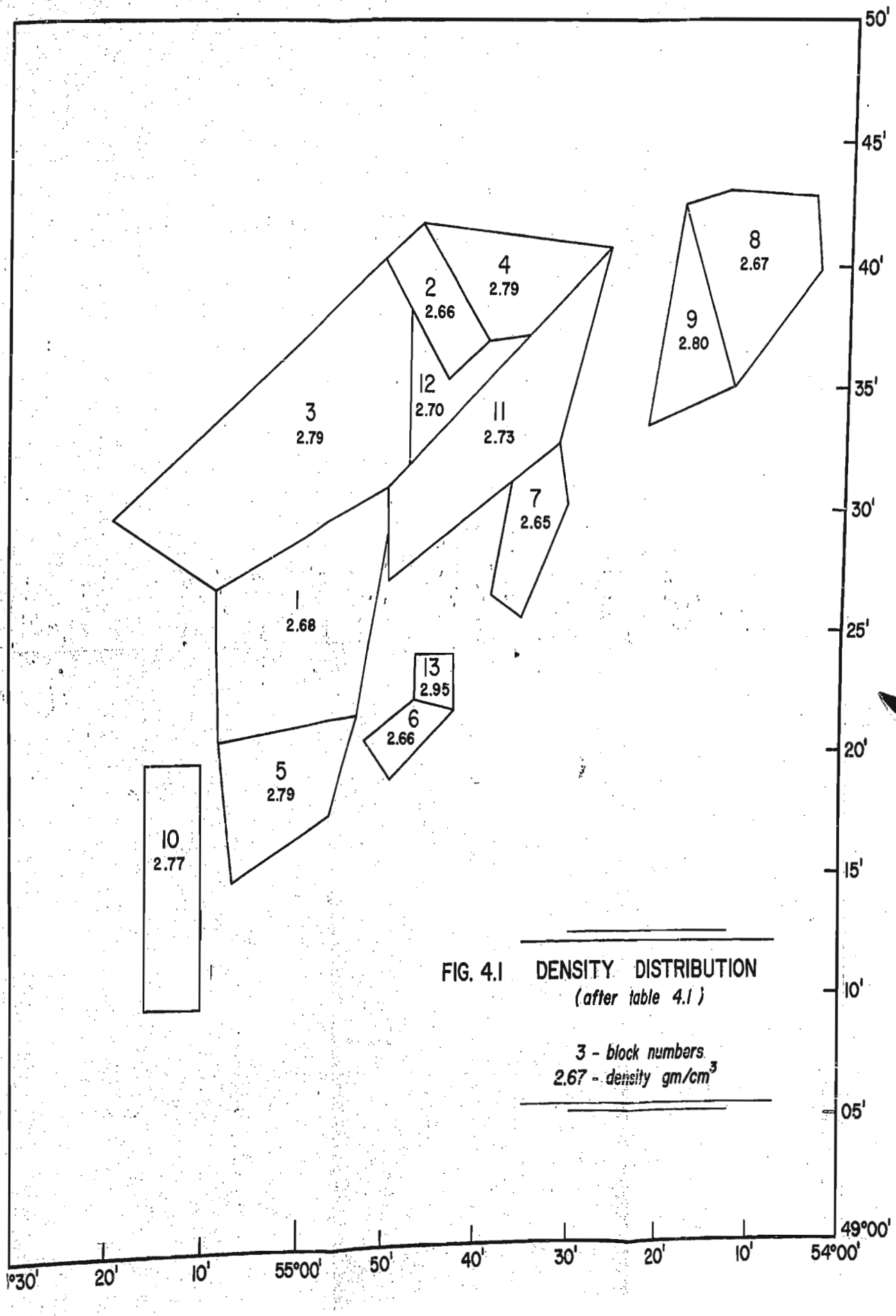

FIG. 4.1 DENSITY DISTRIBUTION
(after table 4.1)

3 - block numbers
2.67 - density gm/cm³

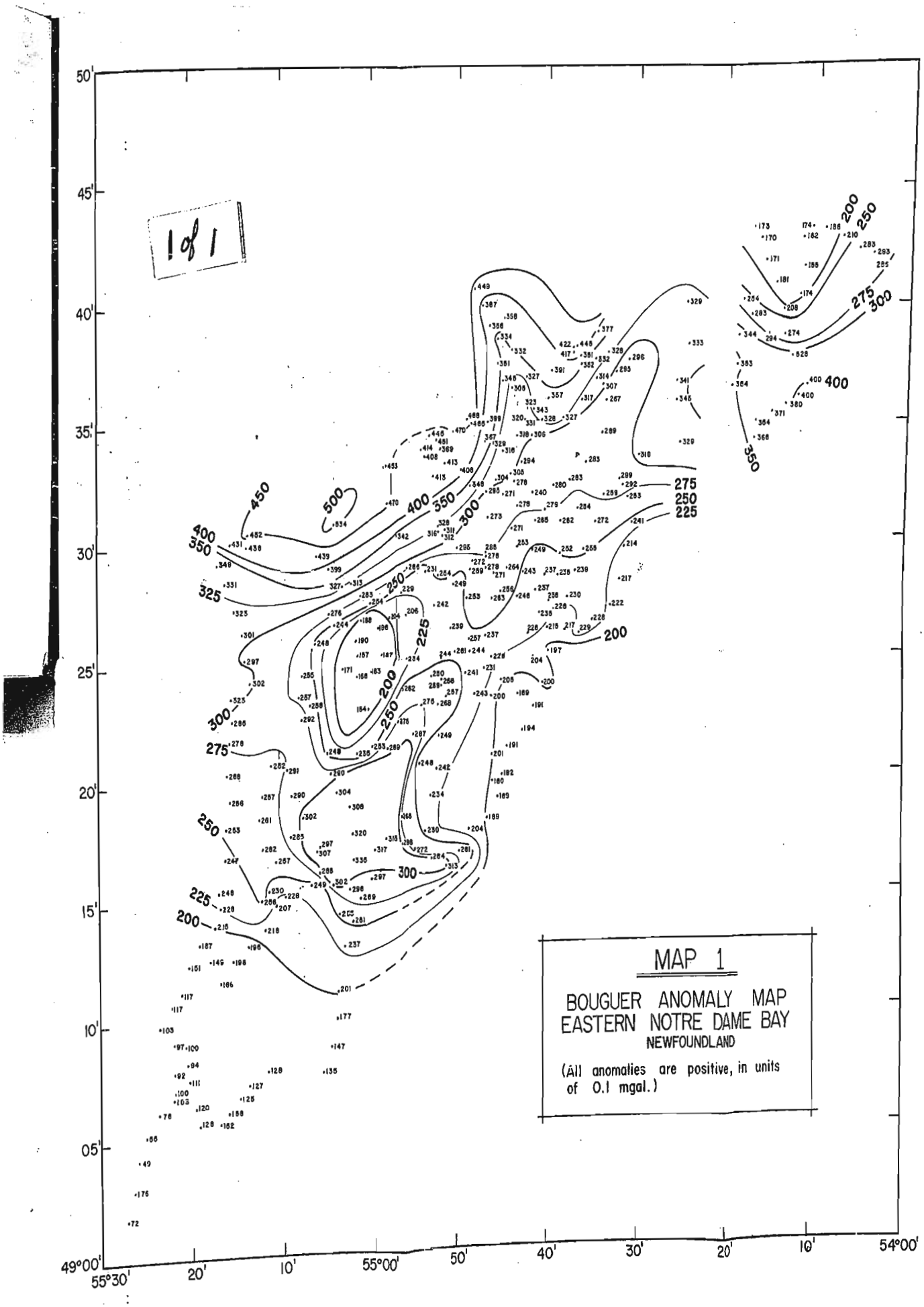
1 of 1
MAP 1
BOUGUER ANOMALY MAP
EASTERN NOTRE DAME BAY
NEWFOUNDLAND
(All anomalies are positive, in units of 0.1 mgal.)
50'
45'
40'
35'
30'
25'
20'
15'
10'
05'
49°00'
55°30'
20'
10'
55°00'
50'
40'
30'
20'
10'
54°00'

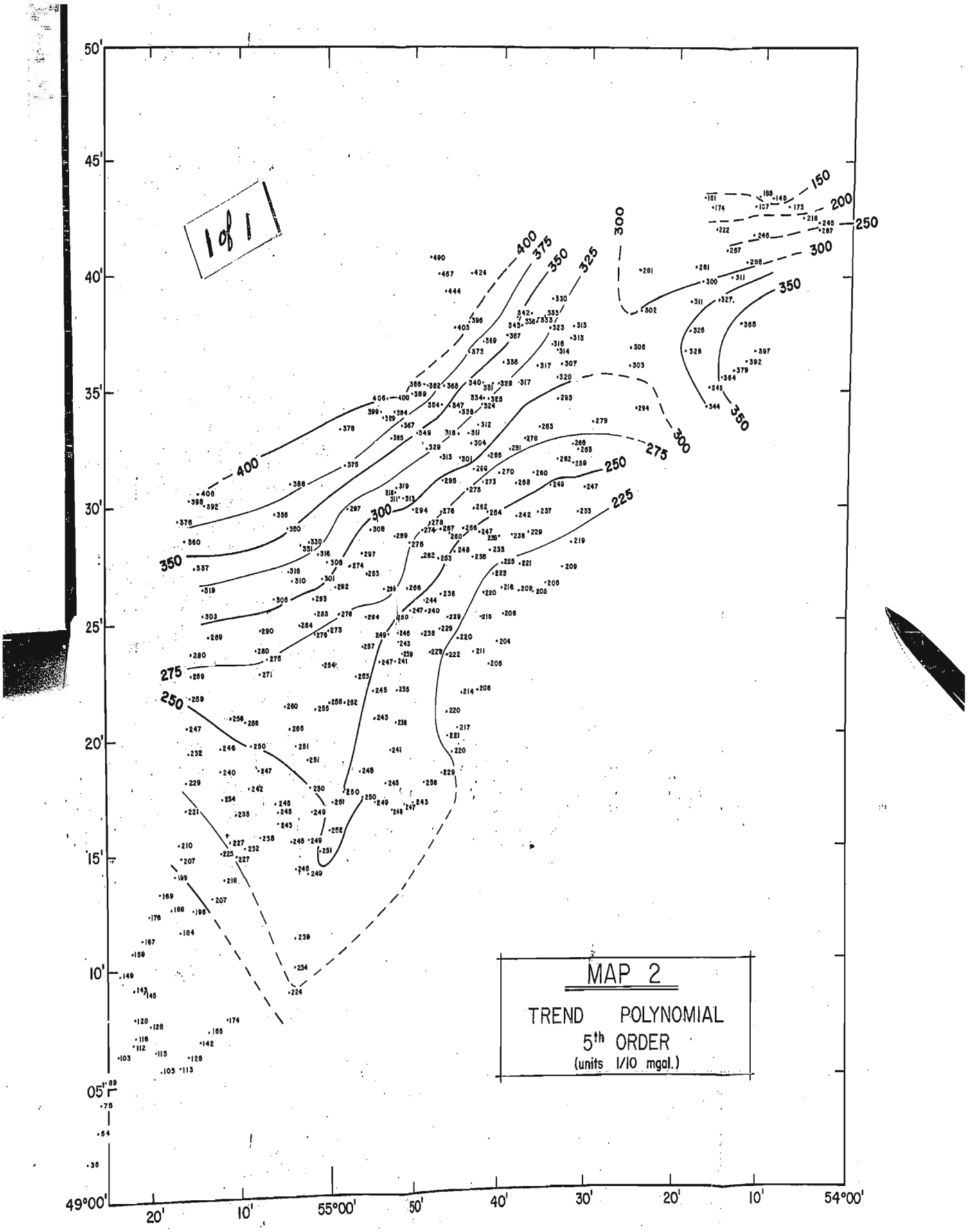
1 of 1
MAP 2
TREND POLYNOMIAL
5th ORDER
(units 1/10 mgal.)
50'
45'
40'
35'
30'
25'
20'
15'
10'
05'
49°00'
20'
10'
55°00'
50'
40'
30'
20'
10'
54°00'

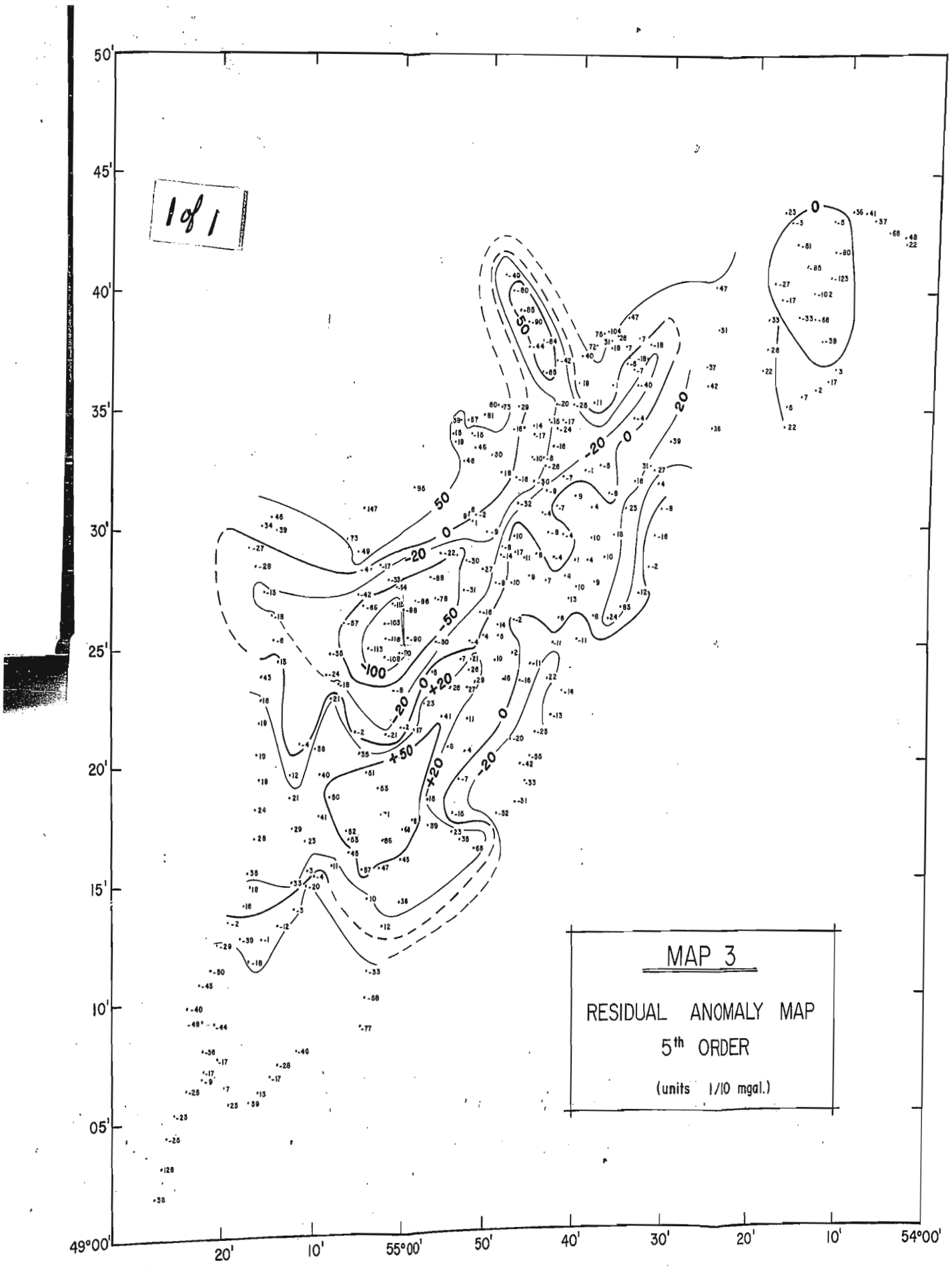
1 of 1
50'
45'
40'
35'
30'
25'
20'
15'
10'
05'
49°00'
20'
10'
55°00'
50'
40'
30'
20'
10'
54°00'
MAP 3
RESIDUAL ANOMALY MAP
5th ORDER
(units 1/10 mgal.)

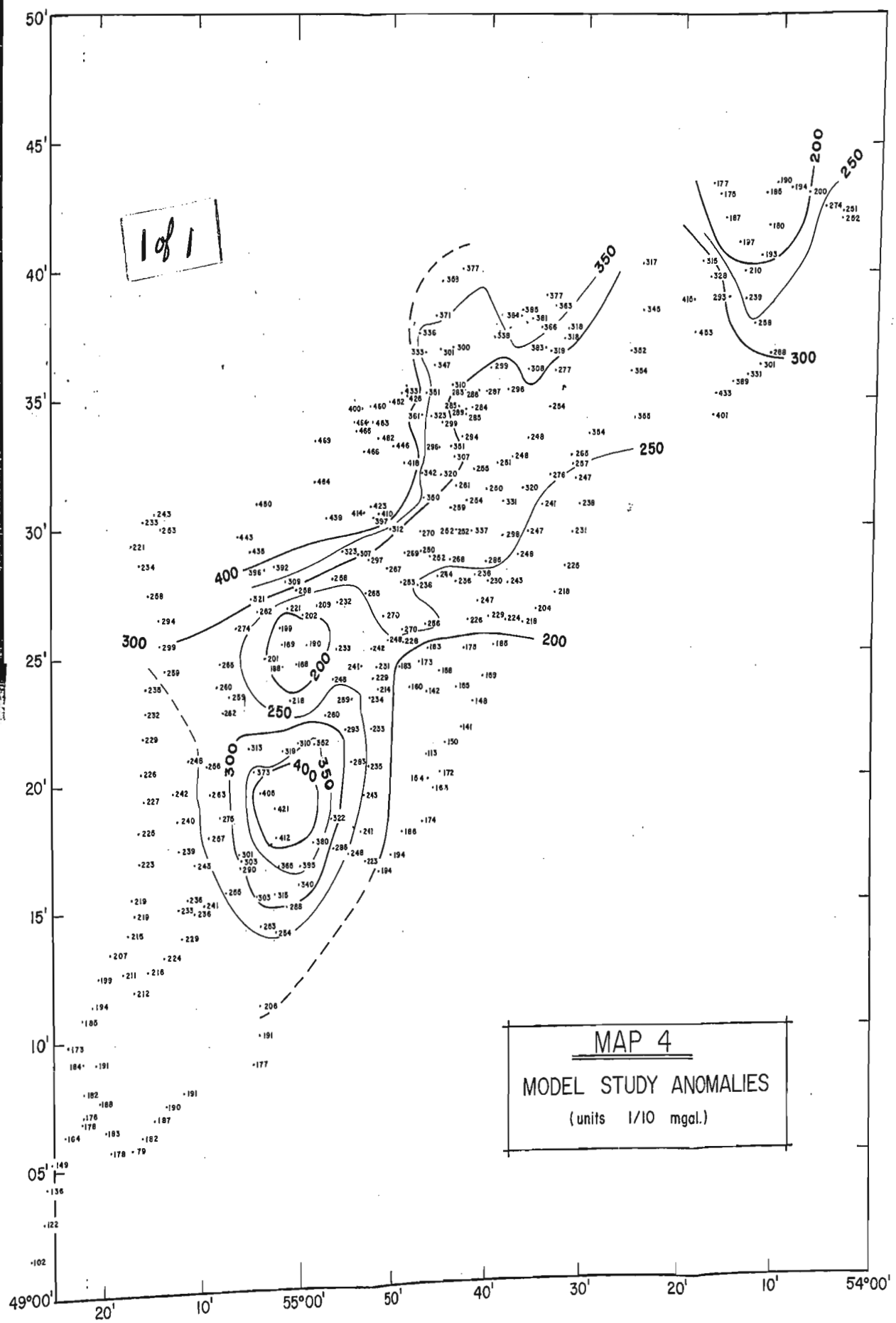
181
MAP 4
MODEL STUDY ANOMALIES
(units 1/10 mgal.)
50'
45'
40'
35'
30'
25'
20'
15'
10'
05'
49°00'
20'
10'
55°00'
50'
40'
30'
20'
10'
54°00'